



**HAL**  
open science

## Cyclitol metabolism is a central feature of Burkholderia leaf symbionts

Bram Danneels, Monique Blignaut, Guillaume Marti, Simon Sieber, Peter Vandamme, Marion Meyer, Aurélien Carlier

► **To cite this version:**

Bram Danneels, Monique Blignaut, Guillaume Marti, Simon Sieber, Peter Vandamme, et al.. Cyclitol metabolism is a central feature of Burkholderia leaf symbionts. *Environmental Microbiology*, 2023, 25 (2), pp.454-472. 10.1111/1462-2920.16292 . hal-04043115

**HAL Id: hal-04043115**

**<https://hal.inrae.fr/hal-04043115>**

Submitted on 27 Nov 2023

**HAL** is a multi-disciplinary open access archive for the deposit and dissemination of scientific research documents, whether they are published or not. The documents may come from teaching and research institutions in France or abroad, or from public or private research centers.

L'archive ouverte pluridisciplinaire **HAL**, est destinée au dépôt et à la diffusion de documents scientifiques de niveau recherche, publiés ou non, émanant des établissements d'enseignement et de recherche français ou étrangers, des laboratoires publics ou privés.

1 TITLE : Cyclitol metabolism is a central feature of *Burkholderia* leaf symbionts

2

3

4 Authors:

5 Danneels, Bram<sup>1,2,\*</sup>, Blignaut, Monique<sup>3</sup>, Marti, Guillaume<sup>4,5</sup>, Sieber, Simon<sup>6</sup>, Vandamme,

6 Peter<sup>1</sup>, Meyer, Marion<sup>3</sup>, Carlier, Aurélien<sup>1,2,\*</sup>

7

8 <sup>1</sup> Laboratory of Microbiology, Department of biochemistry and microbiology, Ghent

9 University, Ghent, Belgium

10 <sup>2</sup> LIPME, Université de Toulouse, INRAE, CNRS, 31320 Castanet-Tolosan, France

11 <sup>3</sup> Department of Plant Science, University of Pretoria, Pretoria, South Africa

12 <sup>4</sup> Metatoul-AgromiX Platform, LRSV, Université de Toulouse, CNRS, UT3, INP, Toulouse,

13 France

14 <sup>5</sup> MetaboHUB-MetaToul, National Infrastructure of Metabolomics and Fluxomics, Toulouse,

15 31077, France

16 <sup>6</sup> Department of Chemistry, University of Zurich, 8057 Zurich, Switzerland.

17 \* Co-corresponding author

18

19 Corresponding authors:

20 Bram Danneels: [bram.danneels@inrae.fr](mailto:bram.danneels@inrae.fr)

21 Aurélien Carlier: [aurelien.carlier@inrae.fr](mailto:aurelien.carlier@inrae.fr)

22

23        *Abstract*

24    The symbioses between plants of the Rubiaceae and Primulaceae families with *Burkholderia*  
25    bacteria represent unique and intimate plant-bacterial relationships. Many of these  
26    interactions have been identified through PCR-dependent typing methods, but there is little  
27    information available about their functional and ecological roles. We assembled seventeen  
28    new endophyte genomes representing endophytes from thirteen plant species, including  
29    those of two previously unknown associations. Genomes of leaf endophytes belonging to  
30    *Burkholderia s.l.* show extensive signs of genome reduction, albeit to varying degrees. Except  
31    for one endophyte, none of the bacterial symbionts could be isolated on standard  
32    microbiological media. Despite their taxonomic diversity, all endophyte genomes contained  
33    gene clusters linked to the production of specialized metabolites, including genes linked to  
34    cyclitol sugar analog metabolism and in one instance non-ribosomal peptide synthesis. These  
35    genes and gene clusters are unique within *Burkholderia s.l.* and are likely horizontally  
36    acquired. We propose that the acquisition of secondary metabolite gene clusters through  
37    horizontal gene transfer is a prerequisite for the evolution of a stable association between  
38    these endophytes and their hosts.

39        *Introduction*

40    Interactions with microbes play an important part in the evolution and ecological success of  
41    plants. For example, mycorrhizal associations are present in a vast majority of land plants,  
42    and the association with nitrogen-fixing bacteria provided legumes with an important  
43    evolutionary advantage (Brundrett, 1991; van Rhijn and Vanderleyden, 1995; Vessey *et al.*,  
44    2005; Smith and Read, 2008). Nevertheless, microbes may also be harmful for plants as  
45    microbial pathogen interactions are responsible for major crop losses (Dangl and Jones,  
46    2001; McCann, 2020). Many plant-microbe interactions only occur temporarily: contacts  
47    between microbes and the host are often limited to a sub-population or a specific  
48    developmental phase of the host. However, in some associations microbes are transferred  
49    from parents to offspring in a process called vertical transmission, resulting in permanent  
50    associations with high potential for co-evolution (Gundel *et al.*, 2017). While vertically-  
51    transmitted microbes are common in the animal kingdom, they have been more rarely  
52    described in plants (Fisher *et al.*, 2017).

53 A particular case of vertically transmitted microbes in plants are the bacterial leaf  
54 endophytes found in three different plant families: the monocot Dioscoreaceae, and the  
55 dicot Rubiaceae and Primulaceae. In the genera *Psychotria*, *Pavetta*, *Sericanthe* (Rubiaceae)  
56 and *Ardisia* (Primulaceae) this association may manifest in the form of conspicuous leaf  
57 nodules that house extracellular symbiotic bacteria (Miller, 1990; Van Oevelen *et al.*, 2002;  
58 Lemaire, Robbrecht, *et al.*, 2011; Lemaire, Van Oevelen, *et al.*, 2012; Ku and Hu, 2014). In  
59 some of these systems, the symbiont was detected in seeds, indicating that they can be  
60 transmitted vertically (Miller I. M., 1987; Sinnesael *et al.*, 2018). Molecular analysis of the  
61 leaf nodules revealed that all endophytes are members of the *Burkholderia sensu lato*, more  
62 specifically to the newly defined *Caballeronia* genus (Van Oevelen *et al.*, 2002; Ku and Hu,  
63 2014). Similar leaf endophytes, also belonging to the *Burkholderiaceae*, are present in  
64 Rubiaceae species that do not form leaf nodules, including some *Psychotria species* (Lemaire,  
65 Lachenaud, *et al.*, 2012; Verstraete *et al.*, 2013). To date, only one symbiont of Rubiaceae  
66 and Primulaceae has been cultivated: the endophyte of *Fadogia homblei*, which has been  
67 identified as *Paraburkholderia caledonica* (Verstraete *et al.*, 2011). Interestingly, members of  
68 *P. caledonica* are also commonly isolated from the rhizosphere or soil and have been  
69 detected in leaves of some *Vangueria* species (Verstraete *et al.*, 2014).

70 Speculations about possible functions of these leaf symbioses have long remained  
71 unsubstantiated because efforts to isolate leaf nodule bacteria or to culture bacteria-free  
72 plants were unsuccessful (Miller, 1990). Recently, sequencing and assembly of leaf symbiont  
73 genomes of several *Psychotria*, *Pavetta* or *Ardisia* species allowed new hypotheses about the  
74 ecological function of leaf symbiosis. Leaf symbiotic *Candidatus Burkholderia crenata*  
75 associated with *Ardisia crenata*, are responsible for the production of FR900359, a cyclic  
76 depsipeptide with potent bioactive and insecticidal properties (Fujioka *et al.*, 1988; Carlier *et*  
77 *al.*, 2016). Similarly, analysis of the genome of *Ca. Burkholderia kirkii* (*Ca. B. kirkii*), the leaf  
78 symbiont of *Psychotria kirkii*, revealed a prominent role of secondary metabolism (Carlier  
79 and Eberl, 2012). In this species, two biosynthetic gene clusters harboured on a plasmid  
80 encode two homologs of a 2-*epi*-5-*epi*-valiolone synthase (EEVS). EEVS are generally required  
81 for the production of cyclitol sugar analogs, a family of bioactive natural products with  
82 diverse targets (Mahmud, 2003, 2009). *Ca. B. kirkii* is likely involved in the synthesis of two  
83 cyclitol metabolites: kirkamide, a C<sub>7</sub>N aminocyclitol with insecticidal properties, and streptol

84 glucoside, a derivative of valienol with broad allelopathic activities (Sieber *et al.*, 2015;  
85 Georgiou *et al.*, 2021). Similarly, representative genomes of *Candidatus Burkholderia*  
86 *humilis*, *Candidatus Burkholderia pumila*, *Candidatus Burkholderia verschuerenii*, *Candidatus*  
87 *Burkholderia brachyanthoides*, *Candidatus Burkholderia calva* and *Candidatus Burkholderia*  
88 *schumanniana* associated with leaf nodules of various *Psychotria* and *Pavetta* species,  
89 encode putative EEVS gene clusters (Pinto-Carbó *et al.*, 2016). The broad conservation of  
90 EEVS in otherwise small genomes suggests that C<sub>7</sub> cyclitol compounds are important for leaf  
91 symbiosis in these species.

92 C<sub>7</sub> cyclitols are a group of natural products derived from the pentose phosphate pathway  
93 intermediate sedoheptulose-7-phosphate (SH7P) (Mahmud, 2003). Proteins of the sugar  
94 phosphate cyclase family are key enzymes in the synthesis of C<sub>7</sub> cyclitols. Enzymes of this  
95 family catalyse the cyclization of sugar compounds, an important step in primary and  
96 secondary metabolism (Wu *et al.*, 2007). Within this family, three main categories of  
97 enzymes use SH7P as a substrate: desmethyl-4-deoxygadusol synthase (DDGS), 2-*epi*-  
98 *valiolone* synthase (EVS) and 2-*epi*-5-*epi*-*valiolone* synthase (EEVS), of which EEVS is the only  
99 known enzyme involved in C<sub>7</sub>N aminocyclitol synthesis (Osborn *et al.*, 2017). EEVS were  
100 originally only found in bacteria, where they catalyse the first step in the biosynthesis of C<sub>7</sub>N  
101 aminocyclitol secondary metabolites (Mahmud, 2003; Sieber *et al.*, 2015). More recently,  
102 EEVS homologs have been discovered in some Eukaryotes such as fish, reptiles, and birds as  
103 well (Osborn *et al.*, 2015, 2017).

104 A second common feature of the leaf endophytes in Rubiaceae and Primulaceae is their  
105 reduced genomes. Leaf nodule *Burkholderia* symbionts of Rubiaceae and Primulaceae  
106 typically have smaller genomes than free-living relatives, as well as a lower coding capacity  
107 (Pinto-Carbó *et al.*, 2016). This reductive genome evolution is thought to be a result of  
108 increased genetic drift sustained in bacteria that are strictly host-associated, which leads to  
109 fixation of deleterious and/or neutral mutations and eventually to the loss of genes  
110 (Pettersson and Berg, 2007). This process is best documented in obligate insect symbionts  
111 such as *Buchnera* and *Serratia*, endosymbionts of aphids, or in *Sodalis*-allied symbionts of  
112 several insect groups (Shigenobu *et al.*, 2000; Toh *et al.*, 2006; Manzano-Marín *et al.*, 2018).  
113 Some of these symbionts have extremely small genomes and may present an extensive  
114 nucleotide bias towards adenosine and thymine (AT-bias) (Moran *et al.*, 2008). The process

115 of genome reduction has multiple stages: first, recently host-restricted symbionts begin  
116 accumulating pseudogenes and insertion elements (McCutcheon and Moran, 2011; Lo *et al.*,  
117 2016; Manzano-Marín and Latorre, 2016). Non-coding and selfish elements eventually get  
118 purged from the genomes over subsequent generations, which together with the general  
119 deletional bias in bacteria results in a decrease in genome size (Mira *et al.*, 2001). This  
120 ultimately leads to symbionts with tiny genomes, retaining only a handful of essential genes  
121 necessary for survival or performing their role in the symbiosis. This process has been well  
122 documented in the leaf nodule symbionts of *Psychotria*, *Pavetta* and *Ardisia* species, but  
123 little is known about the genomes and functions of endophytes in species that do not form  
124 leaf nodules, notably Rubiaceae species of the *Vangueria* and *Fadogia* genera.

125 Here, we performed a comparative study of Rubiaceae and Primulaceae leaf endophytes  
126 from leaf nodulating and non-nodulating plant species using genomes assembled from  
127 shotgun metagenome sequencing data as well as isolates. We constructed a dataset of 26  
128 leaf symbiont genomes (17 of which from this study) from 22 plant species in 5 genera. All  
129 leaf symbionts show signs of genome reduction, in varying degree, and horizontal acquisition  
130 of secondary metabolite clusters is a universal phenomenon in these bacteria.

## 131 *Material and Methods*

### 132 *Sample collection and DNA extraction*

133 Leaves of Rubiaceae and Primulaceae species were freshly collected from different locations  
134 in South Africa or requested from the living collection of botanical gardens (Table S1).  
135 Attempts to isolate the endophytes were made for all fresh samples collected in South Africa  
136 (Table S1). Leaf tissue was surface sterilized using 70% ethanol, followed by manual grinding  
137 of the tissue in 0.4% NaCl. Supernatants were plated on 10% tryptic soy agar medium (TSA,  
138 Sigma) and R2A medium (Oxoid) and incubated at room temperature for 3 days or longer  
139 until colonies appeared. Single colonies were picked and passaged twice on TSA medium.  
140 Isolates were identified by PCR and partial sequencing of the 16S rRNA gene using the pA/pH  
141 primer pair (5'-AGAGTTTGATCCTGGCTCAG and 5'-AAGGAGGTGATCCAGCCGCA) (Edwards *et*  
142 *al.*, 1989). PCR products were sequenced using the Sanger method at Eurofins Genomics  
143 (Ebersberg, Germany). DNA was extracted from whole leaf samples as follows. Whole leaves  
144 were ground in liquid nitrogen using a mortar and pestle. Total DNA was extracted using the

145 protocol of Inglis et al. (Inglis *et al.*, 2018). Total DNA from a *Fadogia homblei* isolate was  
146 extracted following Wilson (Wilson, 2001). Sequencing library preparation and 2x150 paired-  
147 end metagenome sequencing was performed by the Oxford Wellcome Centre for Human  
148 Genetics or by Novogene Europe (Cambridge, UK) using the Illumina NovaSeq 6000.  
149 Sequencing reads were classified using Kraken v2.1.2 against a custom database comprising  
150 complete prokaryotic and plastid genome sequences deposited NCBI RefSeq (accessed  
151 4/4/2021), and visualised using KronaTools v2.7.1 (Ondov *et al.*, 2011; Wood *et al.*, 2019).

### 152 *Isolation of bacteria*

153 Fresh leaf tissue was first washed in running tap water and surface-sterilized for 5 min in a  
154 1.4% solution of sodium hypochlorite followed by 5 min in 70% ethanol. Leaves from a single  
155 plant were processed separately to prevent cross-contamination. Tissue was rinsed in sterile  
156 distilled water twice and ground using a sterile mortar and pestle in aseptic conditions.  
157 Macerates were resuspended in 1 -5 mL of sterile 0.4% NaCl and serial dilutions were spread  
158 onto R2A agar (Reasoner and Geldreich, 1985) and 10% tryptic soy agar (10% TSA; 10%  
159 tryptic soy broth, Oxoid, Thermo Scientific, 18 g L<sup>-1</sup> agar) and incubated at 28°C for a week.  
160 Colonies were picked as they appeared, streaked out on TSA and incubated at room  
161 temperature. Strains were passaged three times on TSA prior to preservation at -80°C in  
162 tryptic soy broth supplemented with 20% glycerol.

### 163 *Bacterial genome assembly*

164 Sequencing reads were trimmed and filtered using fastp v0.21.0 with default settings,  
165 retaining reads with a minimum Phred score of 15 and less than 40% of bases failing the  
166 quality threshold (Chen *et al.*, 2018). Overlapping paired-end reads were merged using  
167 NGmerge v0.3 with default settings (Gaspar, 2018). Reads derived from isolates were  
168 assembled using Skesa v2.4.0 using default settings (Souvorov *et al.*, 2018). Assembly  
169 statistics were compiled using Quast v5.1.0 (Gurevich *et al.*, 2013). For sequencing reads  
170 derived from new leaf samples, metagenome assemblies were created using metaSPAdes  
171 v3.15 on default settings but including the merged reads (Nurk *et al.*, 2017). Metagenomes  
172 were binned using Autometa v1.0.2, using a minimal contig length of 500 bp, taxonomy  
173 filtering (-m) and maximum-likelihood recruitment (using the -r option)(Miller *et al.*, 2019).  
174 Genome bins identified as *Caballeronia*, *Paraburkholderia*, or *Burkholderia* by Autometa

175 were further assembled by mapping the original reads to these bins using smalt v0.7.6  
176 (Ponsting and Ning, 2010). Mapped reads were extracted using samtools v1.9 (Li *et al.*, 2009)  
177 and reassembled using SPAdes v3.15 (Bankevich *et al.*, 2012) in default settings but using the  
178 --careful option, and binned again using Autometa. Contigs likely derived from eukaryotic  
179 contamination were removed after identification by blastn searches (e-value < 1e<sup>-6</sup>) against  
180 the NCBI nucleotide database (accessed January 2021) (Camacho *et al.*, 2009). Per-contig  
181 coverage information was calculated using samtools and contigs with less than 10% or more  
182 than 500% of the average coverage were manually investigated, and sequences likely  
183 derived from other bacterial or eukaryotic genomes were removed. The metagenome  
184 assembly approach was validated using the *Fadogia homblei* PRU 128010 dataset (Table S1)  
185 to compare the *Paraburkholderia caledonica* metagenome-assembled genome (MAG) to the  
186 genome sequence of strain *Paraburkholderia caledonica* R-82532 isolated from the same  
187 source material. MAG sequences of *F. homblei* endophytes contained 100% of the sequences  
188 of the R-82532 isolate genome, with only a small excess of contaminating sequences before  
189 manual filtering (MAG size = 8.90 Mb vs 8.71 Mb for the R-82532 assembly, with 100%  
190 average nucleotide identity on shared sequences).

191 To provide a more homogenous dataset for comparative genomics, Illumina read data for six  
192 previously published Rubiaceae symbionts, and the symbionts of *Ardisia crenata* and  
193 *Fadogia homblei* were re-assembled as above but using the published draft genomes as  
194 trusted contigs for both metaSPAdes and SPAdes assemblies (Table S2). The resulting  
195 assemblies were compared to the published assemblies using dotplots created by MUMmer  
196 v3.1 (Marçais *et al.*, 2018). Genome assemblies of the symbionts of *Psychotria kirkii* (Carlier  
197 and Eberl, 2012; Carlier *et al.*, 2013) and *Psychotria punctata* (Pinto-Carbó *et al.*, 2016) were  
198 downloaded from Genbank (Table S2). To assess whether the (re-)assembled genomes or  
199 MAGs represent new species, genomes were analysed using TYGS (Type Strain Genome  
200 Server) (Meier-Kolthoff and Göker, 2019), and NCBI Blastn-based Average Nucleotide  
201 Identities (ANI) values calculated using the JSpecies web server, accessed Sept. 2021 (Richter  
202 *et al.*, 2016) and the pyANI python package v0.2 (<https://github.com/widdowquinn/pyani>).

### 203 *Genome annotation and pseudogene prediction*

204 Assembled genomes were annotated using the online RASTtk pipeline (Brettin *et al.*, 2015),  
205 using GenemarkS as gene predictor, and locus tags were added using the Artemis software

206 v18.1.0 (Carver *et al.*, 2012). Prediction of pseudogenes was performed using an updated  
207 version of the pseudogene prediction pipeline previously used for leaf symbionts (Carlier *et*  
208 *al.*, 2013). Briefly, orthologs of predicted proteins sequences of each genome in a dataset of  
209 published *Burkholderia* genomes (Table S3) were determined using Orthofinder v2.5.2  
210 (Emms and Kelly, 2019) with default settings. The nucleotide sequences of each gene,  
211 including 200bp flanking regions (the query), were aligned to the highest scoring amino acid  
212 sequence in each orthogroup (the target) using TFASTY v3.6 (Pearson, 2000). Genes were  
213 considered as pseudogenes if the alignment spanned over 50% of the query sequence and  
214 the query nucleotide sequence contained a frameshift, or a nonsense mutation resulting in  
215 an uninterrupted alignment shorter than 80% of the target sequence. Moreover, ORFs were  
216 classified as non-functional if at least one of the following criteria was true: amino acid  
217 sequence shorter than 50 residues which did not cluster in an orthogroup, and sequence  
218 without any significant blastx hit against the reference database (e-value cut off = 0.001);  
219 proteins without predicted orthologs in the *Burkholderia* dataset, but which showed a blastx  
220 hit against the reference set in an alternative reading frame; and finally proteins without any  
221 hit in the *Burkholderia* genome database or in the NCBI nr database. Blastx and blastp  
222 searches were performed using DIAMOND v2 (Buchfink *et al.*, 2021). For the genomes of the  
223 symbionts of *P. kirkii* and *P. punctata* the original gene and pseudogene predictions were  
224 used. Insertion elements in both newly assembled and re-assembled genomes were  
225 predicted using ISEscan v1.7.2.3 with default settings (Xie and Tang, 2017).

## 226 *Phylogenetic analysis*

227 16S rRNA sequences were extracted from the endophyte (meta)genomes using Barrnap v0.9  
228 (<https://github.com/tseemann/barrnap>). For genomes where no complete 16S rRNA could  
229 be detected, reads were mapped to the 16S rRNA gene of the closest relative with a  
230 complete 16S rRNA sequence. These reads were assembled using default SPAdes (Prjibelski  
231 *et al.*, 2020) using the --careful option. Near complete (>95%) 16S rRNA sequences could be  
232 extracted using these methods, except for the hypothetical endophyte of *Pavetta revoluta*.  
233 The 16S rRNA sequences were identified using the EzBiocloud 16S rRNA identification service  
234 (<https://www.ezbiocloud.net/identify>). Phylogenetic analysis of the leaf endophytes and  
235 *Burkholderia s.l.* genomes was performed using the UBCG pipeline v3.0 (Na *et al.*, 2018). The  
236 pipeline was run using the default settings, except for the gap-cutoff (-f 80). The resulting

237 superalignment of 92 core genes was used for maximum-likelihood phylogenetic analysis  
238 using RAxML v8.2.12, using the GTRGAMMA evolution model, and performing 100 bootstrap  
239 replications (Stamatakis, 2014). Plastid reference alignments were created using Realphy  
240 v1.12 using standard settings and the *Coffea arabica* chloroplast genome (NCBI accession  
241 NC\_008535.1) as reference (Bertels *et al.*, 2014). Published chloroplast genomes of *Ardisia*  
242 *mamillata* (NCBI accession MN136062), *Psychotria kirkii* (NCBI accession KY378696), *Pavetta*  
243 *abyssinica* (NCBI accession KY378673), *Pavetta schumanniana* (NCBI Accession MN851271),  
244 and *Vangueria infausta* (NCBI accession MN851269) were also included in the alignment.  
245 Phylogenetic trees were constructed using PhyML v3.3.3 with automatic model selection,  
246 and 1000 bootstrap replicates (Guindon *et al.*, 2010). For plant species with uncertain  
247 taxonomic identification, seven plant markers were extracted by blastn searches against the  
248 metagenome: ITS, nad4, rbcL and rpl16 of *Pavetta abyssinica* (NCBI accessions MK607930.1,  
249 KY492180.1, Z68863.1, and KY378673.1), matK from *Pavetta indica* (NCBI accession  
250 KJ815920.1), petD from *Pavetta bidentata* (NCBI accession JN054223.1), and trnTF from  
251 *Pavetta sansibarica* (NCBI accession KM592134.1).

252 Core-genome phylogenies of symbiont genomes were constructed by individually aligning  
253 the protein sequences of all single-copy core genes using MUSCLE v3.8.1551, back-  
254 translating to their nucleotide sequence using T-Coffee v13.45 (Di Tommaso *et al.*, 2011),  
255 and concatenating all nucleotide alignments into one superalignment using the AlignIO  
256 module of Biopython 1.78 (Cock *et al.*, 2009). Maximum-likelihood phylogenetic analysis was  
257 performed using RAxML, using the GTRGAMMA evolution model, 100 bootstrap replicates,  
258 and using partitioning to allow the model parameters to differ between individual genes.  
259 Phylogenetic trees were visualised and edited using iTOL (Letunic and Bork, 2019).

## 260 *Comparative genomics*

261 Ortholog prediction between leaf symbiont genomes and a selection of reference genomes  
262 of the *Burkholderia*, *Paraburkholderia* and *Caballeronia* genera (BPC-set; selected using NCBI  
263 datasets tool (<https://www.ncbi.nlm.nih.gov/datasets/genomes>); Table S3) was performed  
264 using Orthofinder v2.5.2 using default settings (Emms and Kelly, 2019). For the leaf  
265 endophytes, predicted pseudogenes were excluded from the analysis. The core genome of a  
266 certain group was defined as the number of orthogroups containing genes of all genomes in  
267 the group. Core genome overlap was visualised in Venn diagrams using InteractiVenn

268 (Heberle *et al.*, 2015). Non-essential core genes were identified by blastp searches against  
269 the database of essential genes (DEG)(Zhang, 2004), identifying as putative essential genes  
270 ORFs with significant matches in the database (e-value < 1e<sup>-6</sup>). Standardised functional  
271 annotation was performed using eggNOG-mapper v2.1.2 (Huerta-Cepas *et al.*, 2019;  
272 Cantalapiedra *et al.*, 2021). Enrichment of protein families in leaf symbiont genomes was  
273 determined by comparing the proportion of members of leaf symbionts and the BPC-set in  
274 orthogroups. Enriched KEGG pathways were identified by comparing the average per-  
275 genome counts of genes in every pathway between leaf symbiont genomes and genomes  
276 from the BPC-set. Presence of motility and secretion system clusters was investigated using  
277 the TXSScan models implemented in MacSyFinder (Abby *et al.*, 2014, 2016). Homologues of  
278 the *Ca. B. kirkii* UZHbot1 putative 2-*epi*-5-*epi*-valiolone synthase (EEVS) were identified by  
279 blastp searches against the proteomes of the leaf symbiont genomes (e-value cut-off: 1e<sup>-6</sup>).  
280 Putative EEVS genes were searched against the SwissProt database, and functional  
281 assignment was done by transferring the information from the closest match within the  
282 sugar phosphate cyclase superfamily (Schneider *et al.*, 2004; Osborn *et al.*, 2017). Contigs  
283 containing these genes were identified and extracted using Artemis, and aligned using  
284 Mauve (López-Fernández *et al.*, 2015). Gene phylogenies were constructed by creating  
285 protein alignments using MUSCLE followed by phylogenetic tree construction using FastTree  
286 v2.1.9 (Price *et al.*, 2009), including the protein sequences of three closely related proteins in  
287 other species, determined by blastp searches against the RefSeq protein database (accessed  
288 July 2021). The data generated in this study have been deposited in the European Nucleotide  
289 Archive (ENA) at EMBL-EBI under accession number PRJEB52430  
290 (<https://www.ebi.ac.uk/ena/browser/view/PREJB52430>).

#### 291 *GC-MS analysis of kirkamide*

292 Extracts were derivatised with N-methyl-N-(trimethyl-silyl)-trifluoroacetamide (MSTFA, Merck  
293 Ltd) according to the method of Pinto-Carbó *et al.* (2016). Three replicates of the plant extracts  
294 were derivatised from a concentration of 1 mg/ml in 2 ml double distilled water as follows:  
295 The extracts were filtered through 0.22 µm syringe fitted filters and 100 µl transferred to 2.0  
296 ml screw top glass vials with 200 µl inserts and dried overnight under a nitrogen stream. The  
297 residues were dissolved in 50 µl MSTFA, vortexed for two minutes, left at 70 °C for one hour  
298 and then 50 µl pyridine was added as the solute. The derivatised samples were analysed on a

299 Shimadzu GC-MS-QP2010 (Shimadzu Corporation, Japan) with ionization energy set at 70 eV.  
300 The compounds were separated using a Rtx – 5MS column (29.3 m x 250  $\mu\text{m}$  x 0.25  $\mu\text{m}$  i.d.;  
301 0.25  $\mu\text{m}$  df) with helium as the carrier gas. Splitless injections of 1  $\mu\text{l}$  were performed, with  
302 the column flow set to linear velocity. Sampling time was set to 2 min, with the solvent cut-  
303 off time set to 3.5 min. The injector and interface temperatures were set at 250°C. The GC  
304 oven temperature program was set to an initial 40°C and held for 1 min, thereafter it was  
305 increased to 330°C at a rate of 7°C min<sup>-1</sup> which was held for 10 min, bringing the total run time  
306 to 52 min. The MS ion source and interface temperatures were set to 250°C. The detector  
307 voltage was set to 0.1 kV, relative to the instrument tuning results. The mass-to-charge ratio  
308 ( $m/z$ ) detection was set to start at 7 min (ensuring complete solvent elimination) and ranged  
309 from 45 to 650  $m/z$  with a scan speed of 2 500  $\text{aum s}^{-1}$ . Pyridine was used as a blank at the  
310 start of the analysis to observe any instrumental errors.

#### 311 *UPLC-QToF-MS analysis of streptol and streptol glucoside*

312 The presence of underivatized streptol and streptol glucoside in the plant extracts was  
313 analysed using a Waters Synapt G2 high-definition mass spectrometry (HDMS) system (Waters  
314 Inc., Milford, Massachusetts, USA). The apparatus consists of a Waters Acquity UPLC  
315 connected to a quadrupole-time-of-flight (QToF) instrument. The method of Georgiou et al.  
316 (2021) was followed for the detection of streptol and streptol glucoside in negative mode [ $\text{M}-$   
317  $\text{H}]^-$ . The samples were analysed using a Luna Omega 1.6  $\mu\text{m}$  C<sub>18</sub> 100 A, 100 x 2.1 mm  
318 (Phenomenex, Separations) column and a solvent system that consisted of MeCN:H<sub>2</sub>O (A, 8:2,  
319 0.1 % NH<sub>4</sub>OAc) and MeCN:H<sub>2</sub>O (B, 2:8, 0.1 % NH<sub>4</sub>OAc). The gradient was set to start at 95 % of  
320 B and to decrease to 50 % of B in 7 min, for the next 2 min the gradient was kept at 50 % of B,  
321 the gradient was then gradually decreased from 50 % to 5 % of B for the next 3 min and was  
322 followed by a column wash for the next 2 min giving a total run time of 12 min. The column  
323 temperature was 40 °C, injection volume 7  $\mu\text{l}$  and the flow rate 0.3 ml min<sup>-1</sup>. Mass to charge  
324 ratios ( $m/z$ ) were recorded between 50 and 1 200 Da. High energy collision induced  
325 dissociation (CID) was used for tandem MS fragmentation. The collision energy for the  
326 ramping was set to increase from 10 V to 20 V in order to get a range of data. The full scan MS  
327 data was recorded from the QTOF-MS and XICs (extracted ion chromatograms) were used for  
328 processing the data to single out the ions of interest. In some instances targeted MS/MS  
329 spectra were employed for the detection of streptol. Presence of streptol was determined by

330 the presence of spectral features with ion fragments at 85, 108, 111, 121 and 175  $m/z$  and a  
331 monoisotopic mass of 175.06119 ( $\pm 5$  ppm). Presence of streptol-glucoside was determined  
332 by the presence of spectral features with ion fragments at 112, 139, 175 and 337  $m/z$  and a  
333 monoisotopic mass of 337.1140 ( $\pm 5$  ppm).

334

## 335 *Results*

### 336 *Detection and identification of leaf endophytes*

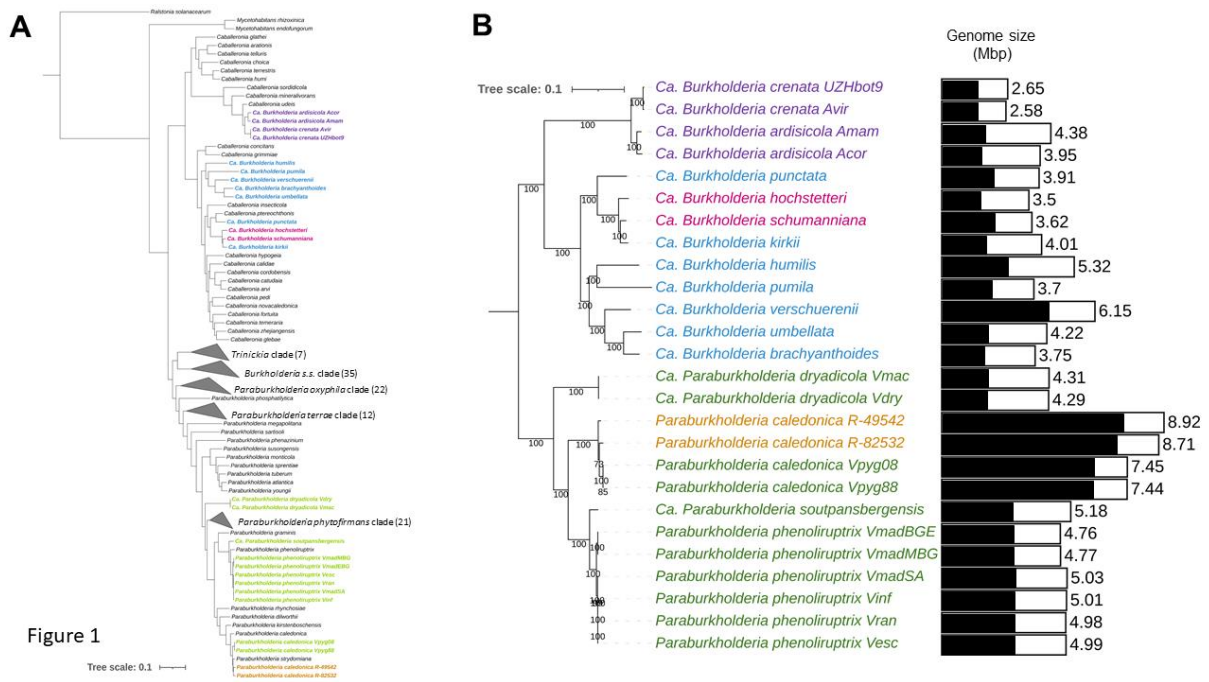
337 To gain insight into potential association of various Primulaceae and Rubiaceae species with  
338 *Burkholderia s.l.* endosymbionts, we collected samples from 16 Rubiaceae (1 *Fadogia* sp., 5  
339 *Pavetta* spp., 2 *Psychotria* spp., and 8 *Vangueria* spp.) and 3 Primulaceae (3 *Ardisia* spp.)  
340 species (Table S1). We extracted DNA from entire leaves and submitted the samples to  
341 shotgun sequencing without pre-processing of the samples to remove host or organellar  
342 DNA. We found evidence for endophytic *Burkholderia* in 14 out of 19 species investigated  
343 (Table S1). In these samples, the proportion of sequencing reads identified as  
344 *Burkholderiaceae* ranged from 5% to 57% of the total, except for the *Pavetta revoluta*  
345 sample (0.4%) and 1 of 2 *Vangueria infausta* samples (0.9%). Analysis of 16S rRNA sequences  
346 revealed 100% pairwise identity over 1529 bp suggesting that the same endophyte species  
347 was present in both *V. infausta* samples. In *Pavetta revoluta*, the closest relative of the leaf  
348 endophyte based on 16S rRNA sequence similarity was *Caballeronia calidae* (98.89% identity  
349 over 808 bp; Table S1). Of the nine species with significant amounts of *Burkholderia s.l.* reads  
350 and for which isolation attempts were made (Table S1), only the endophyte of *Fadogia*  
351 *homblii* could be cultured (isolate R-82532). Leaf samples of four species (*Psychotria*  
352 *capensis*, *Psychotria zombamontana*, *Pavetta ternifolia*, and *Pavetta capensis*) contained low  
353 amounts of bacterial DNA (<2% of reads), and likely do not have stable symbiotic endophyte  
354 associations. Seven percent of the reads obtained from the *Pavetta indica* sample were  
355 classified as bacterial, but with a diverse range of taxa present indicating possible  
356 contamination with surface bacteria (Figure S1). Plastid phylogenies indicated that samples  
357 attributed to *Pavetta capensis* and *Pavetta indica* did not cluster with other *Pavetta* species  
358 (Figure S2). Analysis of genetic markers revealed that our *Pavetta indica* sample was likely a  
359 misidentified *Ixora* species. Analysis of *Pavetta capensis* marker genes revealed the

360 specimen is likely part of the Apocynaceae plant family, with a 100% identity match against  
361 the *rbcl* sequence of *Pleiocarpa mutica*. These samples were not taken into account in  
362 further analyses.

363 Analysis of the 16S rRNA sequences extracted from metagenome-assembled genomes  
364 (MAGs) identified all leaf endophytes as *Burkholderia s.l.* (Table S1). Phylogenetic analysis  
365 shows that all endophytes of *Psychotria*, *Pavetta*, and *Ardisia* cluster within the genus  
366 *Caballeronia*, while the endophytes of *Vangueria* and *Fadogia* belong to the  
367 *Paraburkholderia* genus (Figure 1A). All endophytes of *Ardisia* are closely related to each  
368 other and form a clade with *Caballeronia udeis* and *Caballeronia sordidicola*. Based on the  
369 commonly used ANI (95-96%) cut-off (Richter and Rossello-Mora, 2009), these endophytes  
370 are separate species from *C. udeis* and *C. sordidicola* (ANI <94%; 16S rRNA sequence identity  
371 <98.4). The endophytes of *Ardisia crenata* and *Ardisia virens* are very closely related and  
372 belong to the same species: *Ca. Burkholderia crenata* (ANI >99%; 16S rRNA sequence  
373 identity 99.8%) (Table S4). Similarly, the endophytes of *Ardisia cornudentata* and *Ardisia*  
374 *mamillata* belong to the same species (ANI = 95.56%), which we tentatively named *Ca.*  
375 *Caballeronia ardisicola* (species epithet from *Ardisia*, the genus of the host species, and the  
376 Latin suffix - *cola* (from L. n. *incola*), dweller, see species description in Supplementary  
377 Information). Endophytes of *Psychotria* and *Pavetta* are scattered across the *Caballeronia*  
378 phylogeny, but all are taxonomically distinct from free-living species (Figure 1A; ANI <93%  
379 with closest non-endophyte relatives). Each of these endophytes also represents a distinct  
380 bacterial species with pairwise Average Nucleotide Identity (ANI) values below the  
381 commonly accepted species threshold of 95-96%, including the endophyte of *Pavetta*  
382 *hochstetteri* which we tentatively named *Candidatus Caballeronia hochstetteri* (Table S4 and  
383 Supplementary information). Although their MAGs share 95.65% ANI (a borderline value for  
384 species delineation), *Ca. B. schumanniana* (endophyte of *Pavetta schumanniana*) and *Ca. B.*  
385 *kirkii* have been previously described as distinct species on the basis of 16S rRNA gene  
386 sequence similarity (Verstraete *et al.*, 2011) (Table S4). The endophytes of *Vangueria* and  
387 *Fadogia* form three distinct lineages of *Paraburkholderia*. The endophytes of *Vangueria*  
388 *dryadum* and *Vangueria macrocalyx* are nearly identical (ANI >99.9%; identical 16S rRNA),  
389 but do not belong to any known *Paraburkholderia* species (ANI <83% with closest relative  
390 *Paraburkholderia* species). We tentatively assigned these bacteria to a new species which we

391 named *Ca. Paraburkholderia dryadicola* (from a Dryad, borrowed from the species epithet of  
392 one of the host species, and Latin suffix – *cola*, see species description in Supplementary  
393 Information). Similarly, the endophytes of *V. infausta*, *V. esculenta*, *V. madagascariensis*, *V.*  
394 *randii*, and *V. soutpansbergensis* cluster together with *Paraburkholderia phenoliruptrix*  
395 (Figure 1A). While the endophyte of *Vangueria soutpansbergensis* forms a separate species  
396 (named here *Ca. Paraburkholderia soutpansbergensis*; ANI <95% with *P. phenoliruptrix*) the  
397 other endophytes fall within the species boundaries of *P. phenoliruptrix*. (ANI 95-96%  
398 between these endophytes and *P. phenoliruptrix*). Lastly, the endophytes of *Fadogia homblei*  
399 and *Vangueria pygmaea* showed identical 16S rRNA sequences, and clustered with  
400 *Paraburkholderia caledonica*, *P. strydomiana*, and *P. dilworthii* (Figure 1A). Similarly high ANI  
401 values (>97.5%) and 16S rRNA sequence similarity (>99.7%) ambiguously fall within the  
402 species boundaries of both *P. caledonica* and *P. strydomiana*. Because endophytes of *F.*  
403 *homblei* were previously classified as *P. caledonica* (Verstraete *et al.*, 2011, 2014), we  
404 propose classifying the endophytes of *F. homblei* and *V. pygmaea* as members of *P.*  
405 *caledonica*, and consider *P. strydomiana* a later heterotypic synonym of *P. caledonica*.

406 Phylogenetic analysis based on the core genomes of endophytes indicates a general lack of  
407 congruence with the host plant phylogeny (Figure S3). Endophytes of *Ardisia* are  
408 monophyletic within the *Caballeronia* genus and follow the host phylogeny. In contrast,  
409 endophytes of *Pavetta* are not monophyletic and are nested within the *Psychotria*  
410 endophytes. Similarly, the *Fadogia homblei* endophyte clusters with endophytes of  
411 *Vangueria*.



412

413 **Figure 1: Phylogeny of *Burkholderia*, *Caballeronia*, and *Paraburkholderia*, including the leaf endophytes. (A)**  
 414 UBCG phylogeny of the *Burkholderia* s.l. based on 92 conserved genes. Bootstrap support values based on 100  
 415 replications are displayed on the branches. Branches with <50% support were collapsed. *Ralstonia solanacearum*  
 416 was used as outgroup to root the tree. Coloured samples in boldface represent the leaf endophytes from  
 417 Rubiaceae and Primulaceae (B) Core genome phylogeny of leaf endophytes based on alignment of 423 single-  
 418 copy core genes. Bootstrap support values based on 100 replicates are shown on the branches. Samples are  
 419 colour-coded based on the host genus: Purple – *Ardisia*; Blue – *Psychotria*; Pink – *Pavetta*; Green – *Vangueria*;  
 420 Orange – *Fadogia*; Black bars represent the coding capacity of the genome (the proportion of the genome coding  
 421 for functional proteins).

422

423 *Leaf endophyte genomes show signs of genome reduction.*

424 We could assemble nearly complete bacterial genomes for all samples where we detected  
 425 *Burkholderia* endophytes, except for those of the *Pavetta revoluta* and one *Vangueria*  
 426 *infausta* sample with too few bacterial reads. Binning analysis grouped endophyte  
 427 sequences in a single bin per sample, with high completeness and purity (Table 1). Most  
 428 assemblies ranged between 3.5 and 5 Mbp in size, with 2 outliers: 2.58 Mbp for *Ca. B.*  
 429 *crenata* Avir (the endophyte of *Ardisia virens*), and 8.92 Mbp for *P. caledonica* R-49542  
 430 (endophyte of *Fadogia homblei*)(Table 1). The G+C-content of all MAGs fell in the range of  
 431 59-64 percent G+C content, which is within the range of free-living *Paraburkholderia* and  
 432 *Caballeronia* genomes (Vandamme *et al.*, 2017). All MAGs showed signs of ongoing genome  
 433 reduction. Because of rampant null or frameshift mutations, a large proportion of predicted  
 434 CDS code for non-functional proteins. As a result, coding capacity is low for all endophyte

435 MAGs varying between 83% in *P. caledonica* R-49542 (Figure 1B, Figure S4) and 40% in *Ca. C.*  
436 *ardisicola* Acor, the endophyte of *Ardisia cornudentata* (Figure 1B, Figure S5). In addition,  
437 insertion sequence (IS) elements make up a large amount of the MAGs: 1.97% of the  
438 assembly size on average, but up to almost 10% in some symbionts of *Psychotria* (Table 1).  
439 Reassembly of previously investigated endophytes of *Psychotria* and *Pavetta* yielded  
440 assemblies of similar size to the original assemblies, except for *Ca. Burkholderia*  
441 *schumanniana* UZHbot8 (endophyte of *Pavetta schumanniana*). The original genome  
442 assembly size was estimated at 2.4 Mbp, while our reassembly counted 3.62 Mbp. A dot plot  
443 between both assemblies indicated that the size discrepancy is not solely due to differential  
444 resolution of repeated elements (Figure S6). Thus, our new assembly includes 1.2 Mbp of  
445 genome sequence that was missed in the original assembly.

446 *Burkholderia* leaf endophytes in Rubiaceae and Primulaceae shared a core genome of 607  
447 genes (Figure S7). Even within specific phylogenetic lineages the core genomes were small:  
448 774 genes in endophytes belonging to the *Caballeronia* symbionts of *Psychotria* and *Pavetta*,  
449 1001 genes in endophytes of *Caballeronia* symbionts of *Ardisia*, and 1199 in  
450 *Paraburkholderia* endophytes of *Fadogia* and *Vangueria*. This corresponds to 29.5%, 52.4%,  
451 and 28.4% of the average functional proteome for each species cluster, respectively. Only 28  
452 proteins of the total core genome did not show significant similarity with proteins from the  
453 database of essential genes (Table S5). Eleven of these proteins have unknown functions and  
454 five are membrane-related. Fifteen genes of the endophyte core genome did not have  
455 orthologs in >95% of related *Burkholderia*, *Caballeronia*, and *Paraburkholderia* genomes  
456 (Table S6). No COG category was specifically enriched in this set of proteins.

457 Because secretion of protein effectors is often a feature of endophytic bacteria (Brader *et*  
458 *al.*, 2017), we searched for genes encoding various secretion machineries in the genomes of  
459 *Burkholderia* endophytes. Flagellar genes, as well as Type III, IV or VI secretion system were  
460 not conserved in all leaf endophytes (Figure S8). The most eroded symbionts of *Psychotria*,  
461 *Pavetta*, and *Ardisia* lack almost all types of secretion systems, and most also lack a  
462 functional flagellar apparatus. Type V secretion systems are present in *Ca. Caballeronia*  
463 *ardisicola* Acor, *Ca. B. pumila* UZHbot3 (endophyte of *Psychotria pumila*), and *Ca. B. humilis*  
464 UZHbot5 (endophyte of *Psychotria humilis*). The genomes of *Paraburkholderia* symbionts of  
465 *Vangueria* and *Fadogia* were generally richer in secretions systems, but only T1SS and T2SS

466 are conserved. A Type V secretion system is present in all *Paraburkholderia* endophytes  
467 except *Ca. Paraburkholderia dryadicola* Vdry and Vmac (endophytes of *V. dryadum* and *V.*  
468 *macrocalyx*, respectively). The flagellar apparatus is missing in both *Ca. P. dryadicola* MAGs,  
469 in *Ca. P. soutpansbergensis* Vsou, and in *P. phenoliruptrix* Vesc (the endophyte of *V.*  
470 *esculenta*), and is incomplete in some other *P. phenoliruptrix* endophytes. Lastly, only the  
471 genomes of *Paraburkholderia caledonica* endophytes R-49542 and R-82532 encode a  
472 complete set of core Type VI secretion system proteins.

#### 473 *Genes related to cyclitol metabolism are enriched in leaf endophytes*

474 We wondered if specific metabolic pathways might be enriched in genomes of leaf  
475 symbionts, despite rampant reductive evolution. We assigned KEGG pathway membership  
476 for each predicted functional CDS (thus excluding predicted pseudogenes) in leaf symbiont  
477 genomes or MAGs as well as a set of free-living representative *Paraburkholderia* or  
478 *Caballeronia* species. The number of genes assigned to a majority of the KEGG pathways  
479 (256 pathways in total) was significantly smaller in endophyte genomes compared to their  
480 free-living relatives. A small portion (86 pathways) did not differ between leaf symbionts and  
481 free-living representatives. Genes belonging to a single pathway were significantly enriched  
482 in leaf endophytes: acarbose and validamycin biosynthesis (KEGG pathway map00525).  
483 Acarbose and validamycin are aminocyclitols synthesized via *2-epi-5-epi-valiolone* synthase  
484 (EEVS). EEVS catalyses the first committed step of C<sub>7</sub>N aminocyclitol synthesis (Mahmud,  
485 2003, 2009), and likely plays a role in the production of kirkamide, a natural C<sub>7</sub>N  
486 aminocyclitol present in leaves of *Psychotria kirkii* and other nodulated Rubiaceae, as well as  
487 streptol and streptol glucoside, 2 cyclitols with herbicidal activities (Pinto-Carbó *et al.*, 2016).  
488 Indeed, of 10 *Ca. Burkholderia kirkii* UZHbot1 genes assigned to KEGG pathway map00525, 8  
489 genes were previously hypothesised to play a direct role in the synthesis of C<sub>7</sub>N  
490 aminocyclitol or derived compounds (Pinto-Carbó *et al.*, 2016). Similarly, 7 out of 11  
491 orthogroups most enriched in leaf endophytes contained a gene putatively involved in  
492 cyclitol synthesis in *Ca. Burkholderia kirkii* UZHbot1 (Table S7)(Carlier and Eberl, 2012; Sieber  
493 *et al.*, 2015). To gain a better understanding of the distribution of cyclitol biosynthetic  
494 clusters in leaf endophytes, we searched for homologs of the two *2-epi-5-epi-valiolone*  
495 synthase (EEVS) genes of *Ca. Burkholderia kirkii* UZHbot1 (locus tags BKIR\_C149\_4878 and  
496 BKIR\_C48\_3593) in the other leaf endophyte genomes. We detected putative EEVS

497 homologs in all but the two genomes of *Ca. B. crenata*. For *Ca. B. crenata* UZHbot9 we have  
498 previously shown the genome encodes a non-ribosomal peptide synthase likely responsible  
499 for the synthesis of the depsipeptide FR900359 (Fujioka *et al.*, 1988; Carlier *et al.*, 2016;  
500 Crüsemann *et al.*, 2018), and these genes were also detected in *Ca. B. crenata* Avir. Because  
501 EEVSs are phylogenetically related to 3-dehydroquinate synthases (DHQS), we aligned the  
502 putative EEVS sequences retrieved from leaf endophytes to EEVS and DHQS sequences in the  
503 Swissprot database. All putative EEVS sequences retrieved from leaf endophytic  
504 *Burkholderia* were phylogenetically related to *bona fide* EEVS proteins, but not to  
505 dehydroquinate synthase (DHQS) and other sedoheptulose 7-phosphate cyclases. EEVS are  
506 otherwise rare in *Burkholderia* s. l., with putative EEVSs present in only 11 out of 5674  
507 publicly available *Burkholderiaceae* genomes (excluding leaf symbiotic bacteria) in the NCBI  
508 RefSeq database as of June 2022 (Figure S9).

#### 509 *Evolution of cyclitol metabolism in leaf endophytic Burkholderia*

510 Phylogenetic analysis of the endophyte EEVS protein sequences showed the presence of two  
511 main clades of *Burkholderia* EEVS homologs, as well as a divergent homolog in the genome  
512 of *Ca. C. ardisicola* Acor, and a second divergent homolog in *Ca. P. dryadicola* Vdry and Vmac  
513 (Figure 2A). The gene context of these EEVS genes in the different clades reveals that the  
514 two main EEVS clades correspond to the two conserved gene clusters previously  
515 hypothesized to play a role in kirkamide and streptol glucoside biosynthesis in *Ca.*  
516 *Burkholderia kirkii* (Carlier *et al.*, 2013). The gene order of these clusters is very similar in  
517 every genome, with a similar genomic context in closely related genomes (Tables 2 & 3 and  
518 Figure S10). These gene clusters are generally flanked by multiple mobile elements,  
519 consistent with acquisition via horizontal gene transfer (Table S9). Furthermore, the EEVS  
520 phylogeny did not follow the species phylogeny, indicating that HGT or gene conversion  
521 occurred (Figure 2A and Figure 2B). For clarity, we named the two main putative cyclitol  
522 biosynthetic gene clusters S-cluster (for streptol) and K-cluster (for kirkamide) based on  
523 previous biosynthetic hypotheses from *in silico* analysis of the putative cyclitol gene clusters  
524 of *Ca. B. kirkii* (Figure 2A) (Pinto-Carbó *et al.*, 2016). Both K and S-clusters encode a core set  
525 of proteins linked to sugar analog biosynthesis: a ROK family protein and a HAD family  
526 hydrolase, and both contain aminotransferases (although from different protein families).  
527 Two EEVS genes contain nonsense mutations and are likely not functional: the S-cluster EEVS

528 of *Ca. Burkholderia humilis* UZHbot5, and the K-cluster EEVS of *Ca. Burkholderia*  
529 *brachyanthoides* UZHbot7. The MAG of *Ca. B. humilis* UZHbot5 still contains an apparently  
530 functional K-cluster EEVS, while the pseudogenized EEVS of *Ca. B. brachyanthoides* UZHbot7  
531 is the only homolog in the MAG. Interestingly, genes of the K-cluster appear to be exclusive  
532 to *Psychotria* and *Pavetta* symbionts, while the S-cluster is more widespread, including in the  
533 MAGs of *Vangueria* endophytes. Accordingly, we detected kirkamide in leaf extracts of  
534 *Psychotria kirkii*, but in none of the *Fadogia* or *Vangueria* species we tested (see  
535 supplementary information). We also detected signals that were consistent with  
536 streptol/valienol and streptol glucoside by UPLC-QToF-MS in all samples. However, these  
537 signals occurred in a noisy part of the chromatogram, and we cannot confidently conclude if  
538 these *m/z* features come from a single streptol derivative or from several compounds.

539 The MAG of *Ca. P. soutpansbergensis* Vsou and genomes of *P. caledonica* R-49542 and R-  
540 82532 encoded EEVS homologs of the K-cluster, but the full complement of the genes of the  
541 K-cluster is missing (Table 3 and Figure S10). In both cases the EEVS gene is flanked by IS  
542 elements (Table S9). Accordingly, we did not detect kirkamide in leaf samples from either  
543 *Fadogia homblei* or *V. soutpansbergensis* in our chemical analyses. The MAGs of *Ca. P.*  
544 *dryadicola* Vmac and Vdry encode an EEVS that clusters outside of the K- and S-EEVS  
545 clusters. Genes with putative functions similar to those of the K-cluster are located in the  
546 vicinity of the EEVS in the MAGs of both *Ca. P. dryadicola* strains: oxidoreductases, an  
547 aminotransferase, and an N-acetyltransferase (Table S8). Similarly, *Ca. C. ardisicola* Acor  
548 contains a second divergent EEVS, in addition to the S-cluster EEVS. This EEVS belongs to a  
549 larger gene cluster coding for similar functions also found in the other EEVS-clusters, but  
550 contains at least one frameshift mutation and no longer codes for a functional enzyme  
551 (Table S8). Lastly, *Ca. B. verschuerenii* UZHbot4 contains a second, recently diverged EEVS  
552 paralog of the K-cluster. This EEVS is part of a small cluster of genes, with putative functions  
553 divergent from those found in the other EEVS-clusters and likely does not play a role in  
554 kirkamide synthesis (Table S8).

555

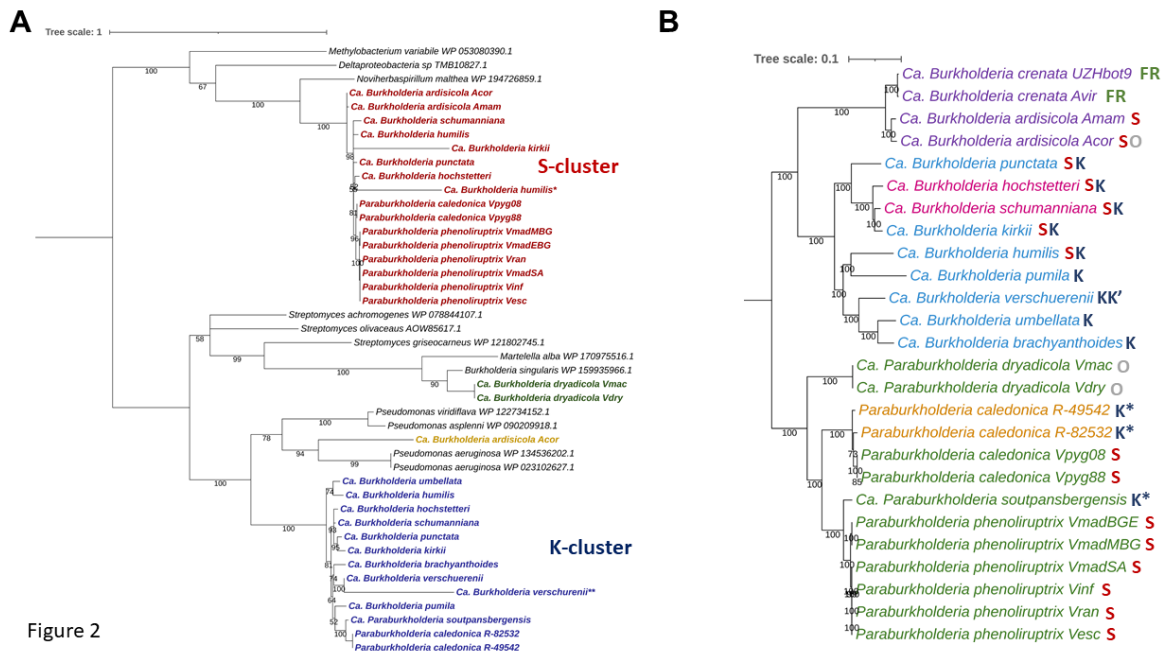


Figure 2

556

557 **Figure 2: EEVS protein phylogeny and distribution in leaf endophytes. (A)** EEVS protein phylogeny of detected  
 558 EEVS-genes and their closest relatives. Local support values based on the Shimodaira-Hasegawa test are shown  
 559 on the branches, and branches with support <50% are collapsed. Coloured samples in boldface are the EEVS  
 560 homologs found in different leaf endophytes. Colours represent different clusters of similar EEVS genes. K- and  
 561 S-cluster are named after their putative products (K for Kirkamide, and S for Streptol glucoside). NCBI accession  
 562 numbers of the close relatives are given next to their species name. The tree is rooted using related 3-  
 563 dehydroquinase synthase genes (not shown). \*The EEVS gene in *Ca. Burkholderia humilis* UZHbot5 contains an  
 564 internal stop codon, creating two EEVS-like pseudogenes. The largest of both was used for the phylogeny. \*\*This  
 565 EEVS gene of *Ca. Burkholderia verschuerenii* UZHbot4 is found outside of the K-cluster. Blue and red labels  
 566 correspond to EEVS sequences belonging to the K and S clusters, respectively. Orange and green labels  
 567 correspond to EEVS sequences found clustering outside of the K and S clusters, the colour corresponding to the  
 568 corresponding taxa as in Figure 1. **(B)** Distribution of specialised metabolism in the leaf endophytes. The  
 569 phylogenetic tree corresponds to the species phylogeny as in Figure 1A. Samples are colour-coded based on the  
 570 host species: Purple – *Ardisia*; Blue – *Psychotria*; Pink – *Pavetta*; Green – *Vangueria*; Orange – *Fadogia*. Codes  
 571 next to the species represent presence of specialised metabolite clusters; FR – FR900359 depsipeptide; K –  
 572 Kirkamide EEVS-cluster; S – Streptol glucoside EEVS-cluster; O – Other EEVS-cluster. K\* – Secondary EEVS cluster  
 573 with EEVS similar to the K-cluster. K\* - Only the K-cluster EEVS is present, not the accessory genes.

574

575 *Discussion*

576 *Different evolutionary origins of leaf symbioses in different plant genera*

577 In this work, we investigated the evolution of associations between *Burkholderia s. l.*  
 578 bacteria and plants of the Rubiaceae and Primulaceae families, and attempted to identify  
 579 key characteristics of these associations. To this end, we re-analyzed publicly available  
 580 genome data from previous research, and sequenced and assembled the genomes of an  
 581 additional 17 leaf endophytes. In addition to leaf endophytes which had been previously

582 detected (Lemaire, Smets, *et al.*, 2011; Verstraete *et al.*, 2011, 2013; Ku and Hu, 2014), we  
583 document here the presence of *Burkholderia s.l.* symbionts in *Pavetta hochstetteri* and  
584 *Vangueria esculenta*, and possibly *Pavetta revoluta*. In contrast to previous findings  
585 (Lemaire, Lachenaud, *et al.*, 2012), we could not detect evidence of leaf endophytes in  
586 *Psychotria capensis*, but did confirm the absence of leaf endophytes in *Psychotria*  
587 *zombamontana*. Phylogenetic placement of hosts and endophytes are consistent with  
588 previous data, except for the placement of *Vangueria macrocalyx* and its endophyte  
589 (Lemaire, Lachenaud, *et al.*, 2012; Verstraete *et al.*, 2013). Both chloroplast sequences of *V.*  
590 *macrocalyx* and *V. dryadum* and the MAGs of their endophytes were nearly identical while  
591 previous research showed a clear phylogenetic difference both between the host species  
592 and their endophytes (Verstraete *et al.*, 2013). Blastn analysis of plant genetic markers (ITS,  
593 petB, rpl16, trnTF) of both species against the NCBI nr database showed higher identities to  
594 markers from *Vangueria dryadum* than to those of *Vangueria macrocalyx*. However, since  
595 comparison of the vouchered *V. macrocalyx* specimen to other vouchered *Vangueria*  
596 *dryadum* and *V. macrocalyx* by expert botanists clearly separated both species, we decided  
597 to consider both species distinct.

598 Previous studies showed that Rubiaceae and Primulaceae species with heritable leaf  
599 symbionts are monophyletic within their respective genera (Lemaire, Vandamme, *et al.*,  
600 2011; Verstraete *et al.*, 2013). Thus, while the transition to a symbiotic state arose  
601 separately in multiple plant genera, it likely evolved only once in each plant genus. The only  
602 exception is the *Psychotria* genus, where it likely arose twice: once in species forming leaf  
603 nodules, and once in species without leaf nodules (Lemaire, Lachenaud, *et al.*, 2012). The  
604 repeated emergence of leaf symbiosis is reflected on the microbial side as well. A  
605 parsimonious interpretation of whole genome phylogenetic analyses indicates that  
606 *Burkholderia* endophytes evolved independently at least 8 times, most probably from  
607 ancestors with an environmental lifestyle (Figure 1A). *Caballeronia* endophytes of *Ardisia*  
608 seem to have emerged once, with most closely related species commonly isolated from soil  
609 (Lim *et al.*, 2003; Vandamme *et al.*, 2013; Uroz and Oger, 2017). As previously reported,  
610 symbionts of *Psychotria* and *Pavetta* cluster in 3 distinct phylogenetic groups within the  
611 *Caballeronia* genus. Finally, symbionts of *Vangueria* and *Fadogia* belong to 5 distinct clades  
612 within the genus *Paraburkholderia*. Apart from *Ca. P. dryadicola* that is without closely

613 related isolates, endophytic *Paraburkholderia* species also cluster together with species  
614 commonly isolated from soil (Verstraete *et al.*, 2014; Beukes *et al.*, 2019). High host-  
615 specificity is a hallmark of the *Psychotria*, *Pavetta*, and *Ardisia* leaf symbiosis, but this  
616 characteristic is not shared in *Vangueria* and *Fadogia*. Based on genome similarity, we  
617 identified at least three phylogenetically divergent endophyte species that can infect  
618 multiple hosts: *P. caledonica*, *P. phenoliruptrix*, and *Ca. P. dryadicola*. It is also possible that  
619 these plants are in the early stages of endophyte capture, where the plant is open to acquire  
620 endophytes from the soil, as previously hypothesized for *F. homblei* (Verstraete *et al.*, 2013).  
621 Endophytes might later evolve to become host-restricted and vertically transmitted, leading  
622 to diversification from their close relatives and forming new species. This could, for example,  
623 already be the case for *Ca. P. soutpansbergensis*, which is related to *P. phenoliruptrix* but  
624 shows a more divergent genome (ANI <95%). Overall, these results highlight the general  
625 plasticity of bacteria in the *Burkholderia s.l.*, as well as the probable frequent occurrence of  
626 host-switching or horizontal transmission within leaf symbiotic associations.

#### 627 *Genome reduction is a common trait of leaf endophytes*

628 Bacterial genomes contain a wealth of information yet few leaf endophyte genomes are  
629 available. In this study we provide an additional thirteen leaf endophyte genome assemblies  
630 among which the first genomes of endophytes from *Vangueria* and *Fadogia*. Aside from the  
631 genomes of *P. caledonica* endophytes, all leaf endophyte genomes were small, mostly  
632 between 3.5 and 5 Mbp. This is well below the average 6.85 Mbp of the *Burkholderiaceae*  
633 family (Carlier *et al.*, 2016; Pinto-Carbó *et al.*, 2016). In addition to their small sizes, the  
634 genomes of *Psychotria*, *Pavetta*, and *Ardisia* endophytes show signs of advanced genome  
635 reduction. Only 41-70% of these genomes code for functional proteins, compared to an  
636 average of about 90% for free-living bacteria (Land *et al.*, 2015). Most of these genomes also  
637 contain a high proportion of mobile sequences, up to 9% of the total assembly. Together,  
638 this indicates ongoing reductive genome evolution, a process often observed in obligate  
639 endosymbiotic bacteria (Moran and Plague, 2004; Bennett and Moran, 2015). Interestingly,  
640 the MAGs of *Vangueria* and *Fadogia* endophytes, which are not contained in leaf nodules,  
641 also show signs of genome erosion: most MAGs of *P. phenoliruptrix* endophytes are at or  
642 below 5 Mbp in size, with over half of their proteome predicted as non-functional. The  
643 genomes of 2 *Ca. P. dryadicola* strains even approach the level of genome reduction found in

644 most *Psychotria* symbionts. The intermediate genome reduction in endophytes of *Vangueria*  
645 and *Fadogia* could be explained by the relatively recent origin of the symbiosis, although leaf  
646 symbiosis in *Fadogia* has been estimated to be older than in *Vangueria* (7.6 Mya vs. 3.7 Mya)  
647 (Verstraete *et al.*, 2017). Other factors likely contribute to the extent or pace of genome  
648 reduction in the endophytes, such as mode of transmission and transmission bottlenecks.  
649 The larger genome size and fewer pseudogenes compared to most other leaf endophytes  
650 may explain why we could isolate *P. caledonica* endophytes from *F. homblei*, but not other  
651 endophytes. We could not identify essential genes or pathways that were consistently  
652 missing in the genomes or MAGs of *Burkholderia* endophytes. It is therefore possible that  
653 other endophytic bacteria may be culturable using more complex or tailored culture  
654 conditions.

#### 655 *Secondary metabolism as key factor in the evolution of leaf symbiosis*

656 Although leaf symbionts share a similar habitat and all belong to the *Burkholderia s. l.*, their  
657 core genome is surprisingly small and consists almost entirely (95%) of genes that are  
658 considered essential for cellular life. This poor conservation of accessory functions perhaps  
659 reflects the large diversity and possible redundancy of functions encoded in the genomes of  
660 *Burkholderia s.l.* that associate with plants. Interestingly, the capacity for production of  
661 secondary metabolites is a key common trait of *Burkholderia* leaf endophytes. We previously  
662 showed that *Ca. B. crenata* produces FR900359, a cyclic depsipeptide isolated from *A.*  
663 *crenata* leaves (Carlier *et al.*, 2016). This non-ribosomal peptide possesses unique  
664 pharmacological properties and may contribute to the protection of the host plant against  
665 insects (Carlier *et al.*, 2016; Crüsemann *et al.*, 2018). However, our data suggests that the  
666 production of cyclitols is widespread in leaf endophytic *Burkholderia*. Indeed, with the  
667 exception of *Ca. B. crenata* cited above, we found evidence for the presence of cyclitol  
668 biosynthetic pathways in all genomes of leaf endophytic *Burkholderia*. We have previously  
669 reported the presence of two gene clusters containing a 2-*epi*-5-*epi*-valiolone synthase  
670 (EEVS) in MAGs of *Psychotria* and *Pavetta* symbionts (Pinto-Carbó *et al.*, 2016). These gene  
671 clusters are likely responsible for the production of 2 distinct cyclitols: kirkamide, a C<sub>7</sub>N  
672 aminocyclitol with insecticidal properties which has been detected in several *Psychotria*  
673 plants; and streptol-glucoside, a plant-growth inhibitor likewise detected in *Psychotria kirkii*  
674 (Sieber *et al.*, 2015; Pinto-Carbó *et al.*, 2016; Hsiao *et al.*, 2019). EEVS from leaf symbionts

675 belong to four phylogenetic clusters, including the two EEVS genes previously detected in  
676 *Psychotria* and *Pavetta* symbionts (Pinto-Carbó *et al.*, 2016). Similar to these previously  
677 analysed leaf endophyte genomes, the EEVS gene clusters in the newly sequenced genomes  
678 are flanked by IS-elements, and their phylogeny is incongruent with the species phylogeny.  
679 This indicates that these genes and clusters are likely acquired via horizontal gene transfer.  
680 This hypothesis is strengthened by the fact that the closest homologs of the genes in the  
681 EEVS clusters are found in genera as diverse as *Pseudomonas*, *Streptomyces*, and  
682 *Noviherbaspirillum*, but are rare in the genomes of *Burkholderia s.l.* The presence of the two  
683 main EEVS gene clusters (K-cluster and S-cluster) is not strictly linked to the symbiont or host  
684 taxonomy. For example, the EEVS of the K-cluster (hypothesised to produce kirkamide) is  
685 present in all sequenced symbionts of *Psychotria* and *Pavetta* but also in the endophytes of  
686 *F. homblei* and *V. soutpansbergensis*. However, in the latter two, accessory genes of the K-  
687 cluster are absent. It is possible that this EEVS interacts with gene products of other  
688 secondary metabolite clusters (Osborn *et al.*, 2017). We also noticed that some endophyte  
689 MAGs contain multiple EEVS genes or gene clusters. This could provide functional  
690 redundancy, protecting against the rampant genome erosion. For example, two genes of the  
691 S-cluster *Ca. C. hochstetteri* PhocE (endophyte of *Pavetta hochstetteri*) are likely  
692 pseudogenes, while the K-cluster gene is still complete. On the other hand, in *Ca.*  
693 *Burkholderia humilis* UZHbot5 (endophyte of *Psychotria humilis*) seven out of ten genes of  
694 the S-cluster (including the EEVS) are either missing or non-functional, and the K-cluster is  
695 heavily reduced with only four functional genes out of eight (including the EEVS). As one  
696 functional EEVS copy remains, it is possible that genes located elsewhere in the genome  
697 provide these functions, as kirkamide has previously been detected in extracts of *P. humilis*  
698 (Pinto-Carbó *et al.*, 2016). Alternatively, this symbiosis may have reached a “point of no  
699 return” where host and symbiont have become dependent on each other and non-  
700 performing symbionts can become fixed in the population (Bennett and Moran, 2015).

701 The presence of gene clusters coding for specialised secondary metabolites in all leaf  
702 symbionts could indicate that secondary metabolite production is either a prerequisite for or  
703 a consequence of an endophytic lifestyle. The fact that *P. caledonica* leaf symbionts have  
704 EEVS genes of different origin favours the hypothesis that the acquisition of secondary  
705 metabolism precedes an endophytic lifestyle. In this case, the ancestor of both endophytes

706 may have acquired differing EEVS genes or EEVS gene clusters through HGT followed by  
707 infection of the respective host plants. The lack of EEVS homolog in *Ca. B. crenata* Avir and  
708 Acre indicates that production of cyclitols is not essential for leaf symbiosis. Interestingly,  
709 MAGs of the sister species *Ca. C. ardisicola* Amam and Acor encode an EEVS and the full S-  
710 cluster complement. Since there is strong phylogenetic evidence of co-speciation in the  
711 *Burkholderia/Ardisia* association (Lemaire, Smets, *et al.*, 2011; Ku and Hu, 2014), the  
712 common ancestor of *Ca. C. ardisicola* and *Ca. B. crenata* possibly possessed both cyclitols  
713 and *frs* pathways, and one of these pathways was lost in the lineages leading to  
714 contemporary *Ca. B. crenata* and *Ca. C. ardisicola*. Alternatively, the genome of the common  
715 ancestor of *Ardisia*-associated *Burkholderia* may have encoded cyclitol S-cluster and later  
716 acquisition of the *frs* gene cluster in the *Ca. B. crenata* lineage alleviated the requirement of  
717 EEVS-related metabolism. The model of horizontal acquisition of secondary functions  
718 supports the model of endophyte evolution described by Lemaire *et al* (Lemaire,  
719 Vandamme, *et al.*, 2011). Different environmental strains which acquired genes for  
720 secondary metabolite production could colonise different host plants in the early open  
721 phase of symbiosis. The different phylogenetic endophyte clades observed in the  
722 *Burkholderia s.l.* phylogeny could each represent distinct acquisitions of secondary  
723 metabolite gene clusters by divergent free-living bacteria followed by colonisation of  
724 different host plants. Many *Burkholderia* species associate with eukaryotic hosts, including  
725 plants (Eberl and Vandamme, 2016), and many of these associations may be transient in  
726 nature. However, useful traits such as synthesis of protective metabolites may help stabilise  
727 these relationships, resulting in long-term associations such as leaf symbiosis.

#### 728 **Author contributions:**

729 AC, MM, and BD designed the research. MM identified and collected wild plant specimens  
730 from the Pretoria region (South Africa). BD, MB, SS, and AC performed the laboratory  
731 experiments and analyses. GM analysed metabolomics data. PV analysed data and made  
732 taxonomic assignments. BD, MM and AC wrote the manuscript with input from all authors.

#### 733 **Acknowledgments**

734 We would like to thank Frédéric De Meyer and Mathijs Deprez for helping with some of the  
735 laboratory experiments. We would further like to thank Steven Janssens (Meise Botanic

736 Garden) and Peter Brownless (Royal Botanic Garden Edinburgh) for facilitating the  
737 acquisition of plant material for this study. BD and AC would like to thank Klaas Vandepoele,  
738 Monica Höfte, Anne Willems and Paul Wilkin for helpful discussion and for proofreading the  
739 manuscript. We also thank Aurélien Bailly (University of Zürich, CH) for providing *P. kirkii*  
740 samples and help with interpreting mass spectrometry data. Magda Nel of the H.G.W.J.  
741 Schweickerdt Herbarium is thanked for her help with plant identification and Mamoalosi  
742 Selepe and Sewes Alberts of the Chemistry and Plant and Soil Sciences Departments,  
743 respectively (University of Pretoria) for chemical analysis. We also thank Chien-Chi Hsiao and  
744 Karl Gademann from University of Zürich (Switzerland) for providing the analytical standards.  
745 This work was supported by the Flemish Fonds Wetenschappelijk Onderzoek under grant  
746 G017717N to AC. AC also acknowledges support from the French National Research Agency  
747 under grant agreement ANR-19-TERC-0004-01 and from the French Laboratory of Excellence  
748 project "TULIP" (ANR-10-LABX-41; ANR-11-IDEX-0002-02) and from the French National  
749 Infrastructure for Metabolomics and Fluxomics, Grant MetaboHUB-ANR-11-INBS-0010. We  
750 thank the Oxford Genomics Centre at the Wellcome Centre for Human Genetics for the  
751 collection and preliminary analysis of sequencing data. The Oxford Genomics Centre at the  
752 Wellcome Centre for Human Genetics is funded by Wellcome Trust grant reference  
753 203141/Z/16/Z. The funders had no role in study design, data collection and analysis,  
754 decision to publish, or preparation of the manuscript.

## 755 **Notes**

756 The authors declare no conflict of interest.

## Tables

**Table 1: Genome statistics of newly assembled and re-assembled leaf endophyte genomes.** Coding capacity refers to the proportion of the genome that codes for functional proteins.

Endophyte	Host species	Type	Assembly size (Mb)	Num. of contigs	N50 (bp)	GC content (%)	Average coverage	Num. of Functional genes	Coding Capacity (%)	Proportion of IS elements(%)	Genome completeness (%)	Genome purity (%)
<i>Ca. Caballeronia ardisicola</i> Acor	<i>Ardisia cornudentata</i>	New assembly	3,95	332	19528	59,23	62x	2026	40,30	0,83	99,28	98,57
<i>Ca. Burkholderia crenata</i> UZHbot9	<i>Ardisia crenata</i>	Re-assembly	2,65	607	6399	59,02	66x	1670	54,73	2,63	95,68	97,08
<i>Ca. Caballeronia ardisicola</i> Amam	<i>Ardisia mamillata</i>	New assembly	4,38	333	19687	59,47	13x	2297	40,95	1,10	96,40	97,10
<i>Ca. Burkholderia crenata</i> Avir	<i>Ardisia virens</i>	New assembly	2,58	605	6517	59,05	13x	1648	56,13	1,64	94,96	99,25
<i>Paraburkholderia caledonica</i> R-49542	<i>Fadogia homblei</i>	Assembly from isolate	8,92	148	145314	61,59	148x	7695	82,83	1,32	100	100
<i>Paraburkholderia caledonica</i> R-82532	<i>Fadogia homblei</i>	Assembly from isolate	8,71	123	239289	61,53	168x	7353	81,03	1,05	100	100
<i>Ca. Caballeronia hochstetteri</i> PhocE	<i>Pavetta hochstetteri</i>	New assembly	3,50	324	18152	62,51	305x	1823	44,53	1,09	99,28	98,57
<i>Ca. Burkholderia schumanniana</i> UZHbot8	<i>Pavetta schumanniana</i>	Re-assembly	3,62	412	14848	63,47	132x	2453	59,95	1,22	100	97,89
<i>Ca. Burkholderia brachyanthoides</i> UZHbot7	<i>Psychotria brachyanthoides</i>	Re-assembly	3,75	648	8356	61,00	121x	2109	46,54	3,98	98,56	98,56
<i>Ca. Burkholderia humilis</i> UZHbot5	<i>Psychotria humilis</i>	Re-assembly	5,32	238	103328	59,60	60x	3264	50,04	1,19	99,28	99,28
<i>Ca. Burkholderia kirkii</i> UZHbot1	<i>Psychotria kirkii</i>	Reference	4,01	203	44916	62,91	196x*	2069	45,80	8,81	99,28	98,57
<i>Ca. Burkholderia pumila</i> UZHbot3	<i>Psychotria pumila</i>	Re-assembly	3,70	463	12628	59,13	110x	2192	45,41	4,15	95,68	98,52
<i>Ca. Burkholderia kirkii</i> UZHbot2	<i>Psychotria punctata</i>	Reference	3,91	48	100248	64,00	-	2539	54,61	9,17	99,28	98,57

<b>Ca. Burkholderia calva</b> <b>UZHbot6</b>	<i>Psychotria</i> <i>umbellata</i>	Re-assembly	4,22	333	28025	61,30	131x	2306	44,37	1,63	98,56	97,86
<b>Ca. Burkholderia verschuerenii</b> <b>UZHbot4</b>	<i>Psychotria</i> <i>verschuerenii</i>	Re-assembly	6,15	401	27267	62,07	39x	4839	70,21	0,99	97,84	98,55
<b>Ca. Paraburkholderia</b> <b>dryadicola Vdry</b>	<i>Vangueria dryadum</i>	New assembly	4,29	153	50748	61,26	67x	2229	43,21	0,82	100	99,29
<b>Paraburkholderia</b> <b>phenoliruptrix Vesc</b>	<i>Vangueria esculenta</i>	New assembly	4,99	180	50333	63,54	160x	3329	59,78	1,09	100	98,58
<b>Paraburkholderia</b> <b>phenoliruptrix Vinf</b>	<i>Vangueria infausta</i>	New assembly	5,00	181	49920	63,51	147x	3320	59,29	1,17	100	98,58
<b>Ca. Paraburkholderia</b> <b>dryadicola Vmac</b>	<i>Vangueria</i> <i>macrocalyx</i>	New assembly	4,31	150	54987	61,30	186x	2243	43,06	0,87	100	99,29
<b>Paraburkholderia</b> <b>phenoliruptrix VmadMBG</b>	<i>Vangueria</i> <i>madagascariensis</i>	New assembly	4,77	247	34361	63,48	79x	3214	61,09	1,15	100	97,20
<b>Paraburkholderia</b> <b>phenoliruptrix VmadEBG</b>	<i>Vangueria</i> <i>madagascariensis</i>	New assembly	4,76	242	34985	63,48	107x	3212	60,97	1,12	100	97,20
<b>Paraburkholderia</b> <b>phenoliruptrix VmadSA</b>	<i>Vangueria</i> <i>madagascariensis</i>	New assembly	5,03	194	50250	63,49	133x	3291	59,22	0,97	100	99,29
<b>Paraburkholderia caledonica</b> <b>Vpyg88</b>	<i>Vangueria pygmaea</i>	New assembly	7,44	92	232014	61,89	35x	6194	82,23	1,00	100	97,20
<b>Paraburkholderia caledonica</b> <b>Vpyg08</b>	<i>Vangueria pygmaea</i>	New assembly	7,45	106	232088	61,90	43x	6193	82,33	1,07	100	97,20
<b>Paraburkholderia</b> <b>phenoliruptrix Vran</b>	<i>Vangueria randii</i>	New assembly	4,98	205	50270	63,33	84x	3294	59,47	1,47	100	98,58
<b>Ca. Paraburkholderia</b> <b>soutpansbergensis Vsou</b>	<i>Vangueria</i> <i>soutpansbergensis</i>	New assembly	5,18	51	337347	63,12	101x	3259	55,24	0,86	99,28	99,28



**Table 3: EEVS K-cluster organisation in endophyte genomes.** Genomes of the same host with the same cluster layout are merged. X: Gene present; -: Gene absent;  $\Psi$ : Gene predicted to be pseudogene; \*: protein overlaps with contig end, other genes of the cluster not found on other contigs; +: Kirkamide detected in leaf extracts of host species; n.t.: not tested;  $\ddagger$  Data from Pinto-Carbo et al. 2016; Abbreviations: EEVS – 2-*epi*-5-*epi*-valiolone synthase. All genes of the cluster were found in the same orientation, with the same order. The gene order is preserved in the table, using the of *Ca. B. kirkii* UZHbot1 accessions as reference.

	GNAT family N-acetyltransferase	Cupin Domain Containing protein	HAD family hydrolase	Gfo/Idh/MocA family oxidoreductase	6-phospho-beta-glucosidase	DegT/DnrJ/EryC1/StrS family aminotransferase	ROK family protein	EEVS	Kirkamide
<b>Reference accessions</b>	CCD36711	CCD36712	CCD36713	CCD36714	CCD36715	CCD36716	CCD6717	CCD36718	
<i>Paraburkholderia caledonica</i> R-49542/R-82532	-	-	-	-	-	-	-	X	-
<i>Ca. Burkholderia brachyanthoides</i> UZHbot7	-	-	-	-	-	-	X/ $\Psi$ *	$\Psi$	- $\ddagger$
<i>Ca. Caballeronia hochstetteri</i> PhocE	X	X	X	X	X	X	X	X	n.t.
<i>Ca. Burkholderia humilis</i> UZHbot5	-	X	$\Psi$	X	X	$\Psi$	X	X	+ $\ddagger$
<i>Ca. Burkholderia kirkii</i> UZHbot1	X	X	X	X	X	X	X	X	+
<i>Ca. Burkholderia pumila</i> UZHbot3	-	X	X	X	X	X	X	X	+ $\ddagger$
<i>Ca. Burkholderia kirkii</i> UZHbot2	X	X	X	X	X	X	X	X	+ $\ddagger$
<i>Ca. Burkholderia schumanniana</i> UZHbot8	X	X	X	X	X	X	X	X	- $\ddagger$
<i>Ca. Burkholderia calva</i> UZHbot6	X	X	X	X	X	X	X	X	- $\ddagger$
<i>Ca. Burkholderia verschuerenii</i> UZHbot4	X	X	X	X	X	X	X	X	+ $\ddagger$
<i>Ca. Paraburkholderia soutpansbergensis</i> Vsou	-	-	-	-	-	-	-	X	n.t.

## References

- Abby, S.S., Cury, J., Guglielmini, J., Néron, B., Touchon, M., and Rocha, E.P.C. (2016) Identification of protein secretion systems in bacterial genomes. *Sci Rep* **6**: 23080.
- Abby, S.S., Néron, B., Ménager, H., Touchon, M., and Rocha, E.P.C. (2014) MacSyFinder: A Program to Mine Genomes for Molecular Systems with an Application to CRISPR-Cas Systems. *PLoS One* **9**: e110726.
- Bankevich, A., Nurk, S., Antipov, D., Gurevich, A.A., Dvorkin, M., Kulikov, A.S., et al. (2012) SPAdes: a new genome assembly algorithm and its applications to single-cell sequencing. *J Comput Biol* **19**: 455–77.
- Bennett, G.M. and Moran, N.A. (2015) Heritable symbiosis: The advantages and perils of an evolutionary rabbit hole. *Proc Natl Acad Sci U S A* **112**: 10169–76.
- Bertels, F., Silander, O.K., Pachkov, M., Rainey, P.B., and van Nimwegen, E. (2014) Automated reconstruction of whole-genome phylogenies from short-sequence reads. *Mol Biol Evol* **31**: 1077–88.
- Beukes, C.W., Steenkamp, E.T., van Zyl, E., Avontuur, J., Chan, W.Y., Hassen, A.I., et al. (2019) *Paraburkholderia strydomiana* sp. nov. and *Paraburkholderia steynii* sp. nov.: rhizobial symbionts of the fynbos legume *Hypocalyptus sophoroides*. *Antonie Van Leeuwenhoek* **112**: 1369–1385.
- Brader, G., Compant, S., Vescio, K., Mitter, B., Trognitz, F., Ma, L.-J., and Sessitsch, A. (2017) Ecology and Genomic Insights into Plant-Pathogenic and Plant-Nonpathogenic Endophytes. *Annu Rev Phytopathol* **55**: 61–83.
- Brettin, T., Davis, J.J., Disz, T., Edwards, R.A., Gerdes, S., Olsen, G.J., et al. (2015) RASTtk: A modular and extensible implementation of the RAST algorithm for building custom annotation pipelines and annotating batches of genomes. *Sci Rep* **5**: 8365.
- Brundrett, M. (1991) Mycorrhizas in Natural Ecosystems. *Adv Ecol Res* **21**: 171–313.
- Buchfink, B., Reuter, K., and Drost, H.-G. (2021) Sensitive protein alignments at tree-of-life scale using DIAMOND. *Nat Methods* **18**: 366–368.
- Camacho, C., Coulouris, G., Avagyan, V., Ma, N., Papadopoulos, J., Bealer, K., and Madden, T.L. (2009) BLAST+: architecture and applications. *BMC Bioinformatics* **10**: 421.
- Cantalapiedra, C.P., Hernandez-Plaza, A., Letunic, I., Bork, P., and Huerta-Cepas, J. (2021) eggNOG-mapper v2: Functional Annotation, Orthology Assignments, and Domain Prediction at the Metagenomic Scale. *Mol Biol Evol* **38**: 5825–5829.
- Carlier, A., Fehr, L., Pinto-Carbó, M., Schäberle, T., Reher, R., Dessein, S., et al. (2016) The genome analysis of *Candidatus Burkholderia crenata* reveals that secondary metabolism may be a key function of the *Ardisia crenata* leaf nodule symbiosis. *Environ Microbiol* **18**: 2507–22.
- Carlier, A.L. and Eberl, L. (2012) The eroded genome of a *Psychotria* leaf symbiont: hypotheses about lifestyle and interactions with its plant host. *Environ Microbiol* **14**: 2757–69.
- Carlier, A.L., Omasits, U., Ahrens, C.H., and Eberl, L. (2013) Proteomics analysis of *Psychotria* leaf nodule symbiosis: improved genome annotation and metabolic predictions. *Mol Plant Microbe Interact* **26**: 1325–33.
- Carver, T., Harris, S.R., Berriman, M., Parkhill, J., and McQuillan, J.A. (2012) Artemis: an integrated platform for visualization and analysis of high-throughput sequence-based experimental data. *Bioinformatics* **28**: 464–469.
- Chen, S., Zhou, Y., Chen, Y., and Gu, J. (2018) fastp: an ultra-fast all-in-one FASTQ preprocessor. *Bioinformatics* **34**: i884–i890.
- Cock, P.J.A., Antao, T., Chang, J.T., Chapman, B.A., Cox, C.J., Dalke, A., et al. (2009) Biopython: freely available Python tools for computational molecular biology and bioinformatics. *Bioinformatics* **25**: 1422–1423.
- Crüsemann, M., Reher, R., Schamari, I., Brachmann, A.O., Ohbayashi, T., Kuschak, M., et al. (2018) Heterologous Expression, Biosynthetic Studies, and Ecological Function of the Selective Gq-Signaling Inhibitor FR900359.

*Angew Chemie Int Ed* **57**: 836–840.

- Dangl, J.L. and Jones, J.D.G. (2001) Plant pathogens and integrated defence responses to infection. *Nature* **411**: 826–833.
- Eberl, L. and Vandamme, P. (2016) Members of the genus *Burkholderia*: good and bad guys. *F1000Research* **5**: 1007.
- Edwards, U., Rogall, T., Blöcker, H., Emde, M., and Böttger, E.C. (1989) Isolation and direct complete nucleotide determination of entire genes. Characterization of a gene coding for 16S ribosomal RNA. *Nucleic Acids Res* **17**: 7843–7853.
- Emms, D.M. and Kelly, S. (2019) OrthoFinder: Phylogenetic orthology inference for comparative genomics. *Genome Biol* **20**: 238.
- Fisher, R.M., Henry, L.M., Cornwallis, C.K., Kiers, E.T., and West, S.A. (2017) The evolution of host-symbiont dependence. *Nat Commun* **8**: 15973.
- Fujioka, M., Koda, S., Morimoto, Y., and Biemann, K. (1988) Structure of FR900359, a cyclic depsipeptide from *Ardisia crenata* Sims. *J Org Chem* **53**: 2820–2825.
- Gaspar, J.M. (2018) NGmerge: merging paired-end reads via novel empirically-derived models of sequencing errors. *BMC Bioinformatics* **19**: 536.
- Georgiou, A., Sieber, S., Hsiao, C.-C., Grayfer, T., Gorenflos López, J.L., Gademann, K., et al. (2021) Leaf nodule endosymbiotic *Burkholderia* confer targeted allelopathy to their *Psychotria* hosts. *Sci Rep* **11**: 22465.
- Guindon, S., Dufayard, J.-F., Lefort, V., Anisimova, M., Hordijk, W., and Gascuel, O. (2010) New algorithms and methods to estimate maximum-likelihood phylogenies: assessing the performance of PhyML 3.0. *Syst Biol* **59**: 307–21.
- Gundel, P.E., Rudgers, J.A., and Whitney, K.D. (2017) Vertically transmitted symbionts as mechanisms of transgenerational effects. *Am J Bot*.
- Gurevich, A., Saveliev, V., Vyahhi, N., and Tesler, G. (2013) QUASt: quality assessment tool for genome assemblies. *Bioinformatics* **29**: 1072–5.
- Heberle, H., Meirelles, G.V., da Silva, F.R., Telles, G.P., and Minghim, R. (2015) InteractiVenn: a web-based tool for the analysis of sets through Venn diagrams. *BMC Bioinformatics* **16**: 169.
- Hsiao, C.-C., Sieber, S., Georgiou, A., Bailly, A., Emmanouilidou, D., Carlier, A., et al. (2019) Synthesis and Biological Evaluation of the Novel Growth Inhibitor Streptol Glucoside, Isolated from an Obligate Plant Symbiont. *Chem - A Eur J* **25**: 1722–1726.
- Huerta-Cepas, J., Szklarczyk, D., Heller, D., Hernández-Plaza, A., Forslund, S.K., Cook, H., et al. (2019) eggNOG 5.0: a hierarchical, functionally and phylogenetically annotated orthology resource based on 5090 organisms and 2502 viruses. *Nucleic Acids Res* **47**: D309–D314.
- Inglis, P.W., Pappas, M. de C.R., Resende, L. V., and Grattapaglia, D. (2018) Fast and inexpensive protocols for consistent extraction of high quality DNA and RNA from challenging plant and fungal samples for high-throughput SNP genotyping and sequencing applications. *PLoS One* **13**: e0206085.
- Ku, C. and Hu, J.-M.M. (2014) Phylogenetic and Cophylogenetic Analyses of the Leaf-Nodule Symbiosis in *Ardisia* Subgenus *Crispardisia* (Myrsinaceae): Evidence from Nuclear and Chloroplast Markers and Bacterial *rrn* Operons. *Int J Plant Sci* **175**: 92–109.
- Land, M., Hauser, L., Jun, S.R., Nookaew, I., Leuze, M.R., Ahn, T.H., et al. (2015) Insights from 20 years of bacterial genome sequencing. *Funct Integr Genomics* **15**: 141–161.
- Lemaire, B., Lachenaud, O., Persson, C., Smets, E., and Dessein, S. (2012) Screening for leaf-associated endophytes in the genus *Psychotria* (Rubiaceae). *FEMS Microbiol Ecol* **81**: 364–72.
- Lemaire, B., Van Oevelen, S., De Block, P., Verstraete, B., Smets, E., Prinsen, E., and Dessein, S. (2012)

- Identification of the bacterial endosymbionts in leaf nodules of Pavetta (Rubiaceae). *Int J Syst Evol Microbiol* **62**: 202–209.
- Lemaire, B., Robbrecht, E., van Wyk, B., Van Oevelen, S., Verstraete, B., Prinsen, E., et al. (2011) Identification, origin, and evolution of leaf nodulating symbionts of Sericanthe (Rubiaceae). *J Microbiol* **49**: 935–41.
- Lemaire, B., Smets, E., and Dessein, S. (2011) Bacterial leaf symbiosis in Ardisia (Myrsinoideae, Primulaceae): molecular evidence for host specificity. *Res Microbiol* **162**: 528–34.
- Lemaire, B., Vandamme, P., Merckx, V., Smets, E., and Dessein, S. (2011) Bacterial Leaf Symbiosis in Angiosperms: Host Specificity without Co-Speciation. *PLoS One* **6**: e24430.
- Letunic, I. and Bork, P. (2019) Interactive Tree Of Life (iTOL) v4: recent updates and new developments. *Nucleic Acids Res* **47**: W256–W259.
- Li, H., Handsaker, B., Wysoker, A., Fennell, T., Ruan, J., Homer, N., et al. (2009) The Sequence Alignment/Map format and SAMtools. *Bioinformatics* **25**: 2078–2079.
- Lim, Y.W., Baik, K.S., Han, S.K., Kim, S.B., and Bae, K.S. (2003) *Burkholderia sordidicola* sp. nov., isolated from the white-rot fungus Phanerochaete sordida. *Int J Syst Evol Microbiol* **53**: 1631–1636.
- Lo, W.S., Huang, Y.Y., and Kuo, C.H. (2016) Winding paths to simplicity: Genome evolution in facultative insect symbionts. *FEMS Microbiol Rev* **40**: 855–874.
- López-Fernández, S., Sonego, P., Moretto, M., Pancher, M., Engelen, K., Pertot, I., and Campisano, A. (2015) Whole-genome comparative analysis of virulence genes unveils similarities and differences between endophytes and other symbiotic bacteria. *Front Microbiol* **6**: 419.
- Mahmud, T. (2009) Progress in aminocyclitol biosynthesis. *Curr Opin Chem Biol* **13**: 161–170.
- Mahmud, T. (2003) The C7N aminocyclitol family of natural products. *Nat Prod Rep* **20**: 137–166.
- Manzano-Marín, A., Coeur d’acier, A., Clamens, A.-L., Orvain, C., Cruaud, C., Barbe, V., and Jousset, E. (2018) A Freeloader? The Highly Eroded Yet Large Genome of the *Serratia symbiotica* Symbiont of *Cinara strobilifera*. *Genome Biol Evol* **10**: 2178–2189.
- Manzano-Marín, A. and Latorre, A. (2016) Snapshots of a shrinking partner: Genome reduction in *Serratia symbiotica*. *Sci Rep* **6**: 32590.
- Marçais, G., Delcher, A.L., Phillippy, A.M., Coston, R., Salzberg, S.L., and Zimin, A. (2018) MUMmer4: A fast and versatile genome alignment system. *PLoS Comput Biol* **14**: e1005944.
- McCann, H.C. (2020) Skirmish or war: the emergence of agricultural plant pathogens. *Curr Opin Plant Biol* **56**: 147–152.
- McCutcheon, J.P. and Moran, N.A. (2011) Extreme genome reduction in symbiotic bacteria. *Nat Rev Microbiol* **10**: 13–26.
- Meier-Kolthoff, J.P. and Göker, M. (2019) TYGS is an automated high-throughput platform for state-of-the-art genome-based taxonomy. *Nat Commun* **10**: 2182.
- Miller I. M., D.A.E. (1987) Location and distribution of symbiotic bacteria during floral development in *Ardisia crispa*. *Plant, Cell Environ* **10**: 715–724.
- Miller, I.J., Rees, E.R., Ross, J., Miller, I., Baxa, J., Lopera, J., et al. (2019) Autometa: automated extraction of microbial genomes from individual shotgun metagenomes. *Nucleic Acids Res* **47**: e57–e57.
- Miller, I.M. (1990) Bacterial Leaf Nodule Symbiosis. *Adv Bot Res* **17**: 163–234.
- Mira, A., Ochman, H., and Moran, N.A.N.A. (2001) Deletional bias and the evolution of bacterial genomes. *Trends Genet* **17**: 589–596.
- Moran, N.A., McCutcheon, J.P., and Nakabachi, A. (2008) Genomics and Evolution of Heritable Bacterial Symbionts. *Annu Rev Genet* **42**: 165–190.

- Moran, N.A. and Plague, G.R. (2004) Genomic changes following host restriction in bacteria. *Curr Opin Genet Dev* **14**: 627–33.
- Na, S.I., Kim, Y.O., Yoon, S.H., Ha, S. min, Baek, I., and Chun, J. (2018) UBCG: Up-to-date bacterial core gene set and pipeline for phylogenomic tree reconstruction. *J Microbiol* **56**: 281–285.
- Nurk, S., Meleshko, D., Korobeynikov, A., and Pevzner, P.A. (2017) metaSPAdes: a new versatile metagenomic assembler. *Genome Res* **27**: 824–834.
- Van Oevelen, S., De Wachter, R., Vandamme, P., Robbrecht, E., and Prinsen, E. (2002) Identification of the bacterial endosymbionts in leaf galls of *Psychotria* (Rubiaceae, angiosperms) and proposal of “*Candidatus Burkholderia kirkii*” sp. nov. *Int J Syst Evol Microbiol* **52**: 2023–7.
- Ondov, B.D., Bergman, N.H., and Phillippy, A.M. (2011) Interactive metagenomic visualization in a Web browser. *BMC Bioinformatics* **12**: 385.
- Osborn, A.R., Almabruk, K.H., Holzwarth, G., Asamizu, S., LaDu, J., Kean, K.M., et al. (2015) De novo synthesis of a sunscreen compound in vertebrates. *Elife* **4**.
- Osborn, A.R., Kean, K.M., Alseud, K.M., Almabruk, K.H., Asamizu, S., Lee, J.A., et al. (2017) Evolution and Distribution of C 7 –Cyclitol Synthases in Prokaryotes and Eukaryotes. *ACS Chem Biol* **12**: 979–988.
- Pearson, W.R. (2000) Flexible Sequence Similarity Searching with the FASTA3 Program Package. In *Bioinformatics Methods and Protocols*. New Jersey: Humana Press, pp. 185–219.
- Pettersson, M.E. and Berg, O.G. (2007) Muller’s ratchet in symbiont populations. *Genetica* **130**: 199–211.
- Pinto-Carbó, M., Sieber, S., Desein, S., Wicker, T., Verstraete, B., Gademann, K., et al. (2016) Evidence of horizontal gene transfer between obligate leaf nodule symbionts. *ISME J* **10**: 2092–2105.
- Ponsting, H. and Ning, Z. (2010) SMALT - A New Mapper for DNA Sequencing Reads. *F1000Posters* **1**: 1.
- Price, M.N., Dehal, P.S., and Arkin, A.P. (2009) FastTree: computing large minimum evolution trees with profiles instead of a distance matrix. *Mol Biol Evol* **26**: 1641–50.
- Prijibelski, A., Antipov, D., Meleshko, D., Lapidus, A., and Korobeynikov, A. (2020) Using SPAdes De Novo Assembler. *Curr Protoc Bioinforma* **70**.
- Reasoner, D.J. and Geldreich, E.E. (1985) A new medium for the enumeration and subculture of bacteria from potable water. *Appl Environ Microbiol* **49**: 1–7.
- van Rhijn, P. and Vanderleyden, J. (1995) The *Rhizobium*-plant symbiosis. *Microbiol Rev* **59**: 124–142.
- Richter, M. and Rossello-Mora, R. (2009) Shifting the genomic gold standard for the prokaryotic species definition. *Proc Natl Acad Sci* **106**: 19126–19131.
- Richter, M., Rosselló-Móra, R., Oliver Glöckner, F., and Peplies, J. (2016) JSpeciesWS: a web server for prokaryotic species circumscription based on pairwise genome comparison. *Bioinformatics* **32**: 929–931.
- Schneider, M., Tognolli, M., and Bairoch, A. (2004) The Swiss-Prot protein knowledgebase and ExPASy: providing the plant community with high quality proteomic data and tools. *Plant Physiol Biochem* **42**: 1013–1021.
- Shigenobu, S., Watanabe, H., Hattori, M., Sakaki, Y., and Ishikawa, H. (2000) Genome sequence of the endocellular bacterial symbiont of aphids *Buchnera* sp. APS. *Nature* **407**: 81–86.
- Sieber, S., Carlier, A., Neuburger, M., Grabenweger, G., Eberl, L., and Gademann, K. (2015) Isolation and Total Synthesis of Kirkamide, an Aminocyclitol from an Obligate Leaf Nodule Symbiont. *Angew Chemie Int Ed* **54**: 7968–7970.
- Sinnesael, A., Eeckhout, S., Janssens, S.B., Smets, E., Panis, B., Leroux, O., and Verstraete, B. (2018) Detection of *Burkholderia* in the seeds of *Psychotria punctata* (Rubiaceae) – Microscopic evidence for vertical transmission in the leaf nodule symbiosis. *PLoS One* **13**: e0209091.
- Smith, S.E. and Read, D. (2008) The symbionts forming arbuscular mycorrhizas. In *Mycorrhizal Symbiosis*. Smith,

- S.E. and Read, D.B.T.-M.S. (eds). London: Elsevier, pp. 13–41.
- Souvorov, A., Agarwala, R., and Lipman, D.J. (2018) SKESA: strategic k-mer extension for scrupulous assemblies. *Genome Biol* **19**: 153.
- Stamatakis, A. (2014) RAxML version 8: A tool for phylogenetic analysis and post-analysis of large phylogenies. *Bioinformatics* **30**: 1312–1313.
- Toh, H., Weiss, B.L., Perkin, S.A.H., Yamashita, A., Oshima, K., Hattori, M., and Aksoy, S. (2006) Massive genome erosion and functional adaptations provide insights into the symbiotic lifestyle of *Sodalis glossinidius* in the tsetse host. *Genome Res* **16**: 149–156.
- Di Tommaso, P., Moretti, S., Xenarios, I., Orobítg, M., Montanyola, A., Chang, J.M., et al. (2011) T-Coffee: A web server for the multiple sequence alignment of protein and RNA sequences using structural information and homology extension. *Nucleic Acids Res* **39**: W13-7.
- Uroz, S. and Oger, P. (2017) *Caballeronia mineralivorans* sp. nov., isolated from oak-*Scleroderma citrinum* mycorrhizosphere. *Syst Appl Microbiol* **40**: 345–351.
- Vandamme, P., De Brandt, E., Houf, K., Salles, J.F., van Elsas, J.D., Spilker, T., and LiPuma, J.J. (2013) *Burkholderia humi* sp. nov., *Burkholderia choica* sp. nov., *Burkholderia telluris* sp. nov., *Burkholderia terrestris* sp. nov. and *Burkholderia udeis* sp. nov.: *Burkholderia glathei*-like bacteria from soil and rhizosphere soil. *Int J Syst Evol Microbiol* **63**: 4707–4718.
- Vandamme, P., Peeters, C., De Smet, B., Price, E.P., Sarovich, D.S., Henry, D.A., et al. (2017) Comparative Genomics of *Burkholderia singularis* sp. nov., a Low G+C Content, Free-Living Bacterium That Defies Taxonomic Dissection of the Genus *Burkholderia*. *Front Microbiol* **8**: 1679.
- Verstraete, B., Van Elst, D., Steyn, H., Van Wyk, B., Lemaire, B., Smets, E., and Dessein, S. (2011) Endophytic Bacteria in Toxic South African Plants: Identification, Phylogeny and Possible Involvement in Gousiekte. *PLoS One* **6**: e19265.
- Verstraete, B., Janssens, S., and Rønsted, N. (2017) Non-nodulated bacterial leaf symbiosis promotes the evolutionary success of its host plants in the coffee family (Rubiaceae). *Mol Phylogenet Evol* **113**: 161–168.
- Verstraete, B., Janssens, S., Smets, E., and Dessein, S. (2013) Symbiotic  $\beta$ -Proteobacteria beyond Legumes: *Burkholderia* in Rubiaceae. *PLoS One* **8**: e55260.
- Verstraete, B., Peeters, C., van Wyk, B., Smets, E., Dessein, S., and Vandamme, P. (2014) Intraspecific variation in *Burkholderia caledonica*: Europe vs. Africa and soil vs. endophytic isolates. *Syst Appl Microbiol* **37**: 194–9.
- Vessey, J.K., Pawlowski, K., and Bergman, B. (2005) Root-based N<sub>2</sub>-fixing Symbioses: Legumes, Actinorhizal Plants, Parasponia sp. and Cycads. *Plant Soil* **274**: 51–78.
- Wilson, K. (2001) Preparation of Genomic DNA from Bacteria. *Curr Protoc Mol Biol* **56**: 2.4.1-2.4.5.
- Wood, D.E., Lu, J., and Langmead, B. (2019) Improved metagenomic analysis with Kraken 2. *Genome Biol* **20**: 257.
- Wu, X., Flatt, P.M., Schlörke, O., Zeeck, A., Dairi, T., and Mahmud, T. (2007) A Comparative Analysis of the Sugar Phosphate Cyclase Superfamily Involved in Primary and Secondary Metabolism. *ChemBioChem* **8**: 239–248.
- Xie, Z. and Tang, H. (2017) ISEScan: automated identification of insertion sequence elements in prokaryotic genomes. *Bioinformatics* **33**: 3340–3347.
- Zhang, R. (2004) DEG: a database of essential genes. *Nucleic Acids Res* **32**: 271D – 272.